



ELSEVIER

Available online at www.sciencedirect.com

SCIENCE @ DIRECT®

NUCLEAR
PHYSICS B

Nuclear Physics B 660 (2003) 81–115

www.elsevier.com/locate/npe

D-branes and the Standard Model

I. Antoniadis^{a,1}, E. Kiritsis^{b,d}, J. Rizos^c, T.N. Tomaras^b

^a *CERN Theory Division, CH-1211, Genève 23, Switzerland*

^b *Department of Physics and Institute of Plasma Physics, University of Crete and FORTH,
71003 Heraklion, Greece*

^c *Department of Physics, University of Ioannina, 45110 Ioannina, Greece*

^d *CPHT, UMR du CNRS 7644, Ecole Polytechnique, 91128 Palaiseau, France*

Received 26 November 2002; received in revised form 24 February 2003; accepted 25 March 2003

Abstract

We perform a systematic study of the Standard Model embedding in a D-brane configuration of type I string theory at the TeV scale. We end up with an attractive model and we study several phenomenological questions, such as gauge coupling unification, proton stability, fermion masses and neutrino oscillations. At the string scale, the gauge group is $U(3)_{\text{color}} \times U(2)_{\text{weak}} \times U(1)_1 \times U(1)_{\text{bulk}}$. The corresponding gauge bosons are localized on three collections of branes; two of them describe the strong and weak interactions, while the last Abelian factor lives on a brane which is extended in two large extra dimensions with a size of a few microns. The hypercharge is a linear combination of the first three $U(1)$'s. All remaining $U(1)$'s get masses at the TeV scale due to anomalies, leaving the baryon and lepton numbers as (perturbatively) unbroken global symmetries at low energies. The conservation of baryon number assures proton stability, while lepton number symmetry guarantees light neutrino masses that involve a right-handed neutrino in the bulk. The model predicts the value of the weak angle which is compatible with the experiment when the string scale is in the TeV region. It also contains two Higgs doublets that provide tree-level masses to all fermions of the heaviest generation, with calculable Yukawa couplings; one obtains a naturally heavy top and the correct ratio m_b/m_τ . We also study neutrino masses and mixings in relation to recent solar and atmospheric neutrino data.

© 2003 Elsevier Science B.V. All rights reserved.

E-mail address: irizos@cc.uoi.gr (J. Rizos).

¹ On leave of absence from CPHT, UMR du CNRS 7644, Ecole Polytechnique, 91128 Palaiseau, France.

1. Introduction

In a previous work [1,2], a minimal embedding of the Standard Model (SM) was proposed in a D-brane configuration of type I string theory with large internal dimensions and low fundamental scale [3,4]. The $SU(3)$ color and $SU(2)$ weak gauge fields were confined on two different collections of branes. The model correctly accommodated the right value of the weak angle for a choice of the string scale of a few TeV. It contained two Higgs doublets and guaranteed proton stability. Among the issues, which were not addressed, are the fermion masses, neutrino oscillations, and a natural suppression of lepton number violating processes.

A generic feature of the models studied was that some of the SM states should correspond to open strings with one end in the bulk, implying the existence of some extra branes, in addition to the ones used above [1,2]. Starting from the last point, in the present work we introduce an extra brane in the bulk with a corresponding $U(1)_b$ bulk gauge group [2]. This group is broken by anomalies, leaving behind an additional global symmetry that will be identified with the lepton number. In order to give masses to the neutrinos, we introduce a right-handed neutrino in the bulk [5] that carries non-trivial lepton number. Large neutrino masses are then forbidden by symmetry, while the right-neutrino coupling suppression required to explain the neutrino oscillation data, is achieved if the bulk has two dimensions of submillimeter size.

More precisely, in the minimal case of one bulk neutrino, we show that solar and atmospheric neutrino data can be accommodated using essentially the two lowest frequencies of the neutrino mass matrix: the mass of the zero mode, arising via the electroweak Higgs phenomenon, which is suppressed by the volume of the bulk, and the mass of the first Kaluza–Klein (KK) excitation. The former is used to reproduce the large mixing angle (LMA or even LOW) solution to the solar neutrino anomaly, through $\nu_e \leftrightarrow \nu_\mu$ transitions. The later is used to explain atmospheric neutrino oscillations with an amplitude which is enhanced due to logarithmic corrections of the two-dimensional bulk [6]. Compatibility of the two conditions using one bulk right neutrino is possible only if one introduces a non-orthogonal angle between the two compact bulk dimensions, that leads simultaneously to a CP violation in the neutrino sector. Atmospheric oscillations contain however a significant sterile component which seems to be in contradiction with recent atmospheric data analyses.

We also compute the tree-level Yukawa couplings of the two higgses to the fermions of the heaviest generation. They are given in terms of the gauge couplings and lead to a naturally heavy top and a ratio m_b/m_τ compatible with the experimental data. Next, we proceed to a systematic description of the main features that we will use in the following sections.

The general framework is type I string theory. We shall restrict ourselves to models in which the closed string sector is supersymmetric, while supersymmetry is generically broken by the open strings at the string scale [7].² Within our framework, the minimal ensemble of D-branes needed in our construction is the following mutually orthogonal

² Recent progress in constructing type I vacua with structure close to the SM can be found in [8–10].

stacks: a stack of three coincident branes to generate the color group, a second stack of two coincident branes to describe the weak $SU(2)_L$ gauge bosons, and one more brane to generate the $U(1)_b$ bulk discussed above. The resulting gauge group so far is $U(3)_c \times U(2)_L \times U(1)_b$, with the three $U(1)$ generators denoted by Q_c , Q_L and Q_b , respectively. To ensure proton stability, we require baryon number conservation with generator $B \equiv Q_c$. The hypercharge Y cannot have a component along Q_b , since this would lead to unrealistically small gauge coupling, and as explained in [1] the correct assignment of SM quantum numbers requires the presence of an extra abelian factor, named $U(1)_1$ with generator Q_1 , living on an additional brane. This brane should lie on top of the color or the weak stack of branes, as we argue below.

Since in our framework, supersymmetry is broken by combinations of (anti-)branes and orientifolds which preserve different subsets of the bulk supersymmetries, any pair of D-branes Dp and Dp' satisfy $p - p' = 0 \pmod{4}$. It follows that a system with three stacks of mutually orthogonal branes in the six-dimensional internal (compact) space consists, up to T-dualities, of D9-branes with two different types of D5-branes, extended in different directions. Specifically, the $U(1)_b$ lives on the D9-brane, while the $U(3)_c$ and $U(2)_L$ are confined on two stacks of 5-branes, the first along say the 012345 and the other along the 012367 directions of ten-dimensional spacetime. Thus, the (submillimeter) bulk is necessarily two-dimensional (extended along the 89 directions), and the additional $U(1)_1$ brane has to coincide with either $U(3)_c$ or $U(2)_L$. The parameters of the model are the string scale M_s , the string coupling g_s and the volumes v_{45} , v_{67} and v_{89} of the corresponding subspaces, in string units.³ In terms of those, the four-dimensional Planck mass M_P is given by

$$M_P^2 = \frac{8}{g_s^2} v_{45} v_{67} v_{89} M_s^2 \tag{1.1}$$

and the non-Abelian gauge couplings are

$$\frac{1}{g_3^2} = \frac{1}{g_s} v_{45}, \quad \frac{1}{g_2^2} = \frac{1}{g_s} v_{67}. \tag{1.2}$$

It follows that

$$M_P^2 = \frac{8}{g_3^2 g_2^2} v_{89} M_s^2 = \frac{2}{\alpha_3 \alpha_2} \hat{v}_{89} M_s^2, \tag{1.3}$$

where $\alpha_i = g_i^2/4\pi$ and $\hat{v}_{89} \equiv v_{89}/(2\pi)^2 = R_8 R_9$ for a rectangular torus of radii R_8, R_9 . The $U(1)_1$ gauge coupling g_1 is equal to g_3 (g_2), if the $U(1)_1$ brane is on top of the $U(3)_c$ ($U(2)_L$).

Upon T-duality, one finds two additional realizations: (i) a set of D3-branes (along 0123) describing $U(3)_c$, and two orthogonal sets of D7-branes along 01236789 and 01234567 describing $U(1)_b$ and $U(2)_L$, respectively; (ii) three sets of D5-branes along 012389, 012345 and 012367, giving rise to $U(1)_b$, $U(3)_c$ and $U(2)_L$, respectively. In both cases, relation (1.3) remains intact.

³ Using T-duality, we choose all internal volumes to be bigger than unity, $v_{ij} > 1$.

The gauge coupling g_b of the $U(1)_b$ gauge boson which lives in the bulk is extremely small since it is suppressed by the volume of the bulk v_{89} . For instance, in the case where the $U(1)_b$ lives on a D9-brane, its coupling is given by

$$\frac{1}{g_b^2} = \frac{1}{g_s} v_{45} v_{67} v_{89} = \frac{g_s}{8} \frac{M_P^2}{M_s^2}, \quad (1.4)$$

where in the second equality we used Eq. (1.1). Using now the weak coupling condition $g_s < 1$ and the inequality $g_s > g_{3,2}^2$ following from $v_{ij} > 1$ in Eq. (1.2), one finds

$$\sqrt{8} \frac{M_s}{M_P} < g_b < \frac{\sqrt{8}}{g_3} \frac{M_s}{M_P}, \quad (1.5)$$

which implies that $g_b \simeq 10^{-16} - 10^{-14}$ for $M_s \sim 1 - 10$ TeV.

If the $U(1)_b$ gauge boson is light, it will be subject to strong constraints coming from supernova observations, since it would be copiously produced in various nuclear reactions leading to supernova cooling through energy loss in the bulk of extra dimensions. The corresponding process is much stronger than the production of gravitons because of the non-derivative coupling of the gauge boson interaction [11]. In fact, in the case of n large transverse dimensions of common radius R , satisfying $m_A, R^{-1} \ll T$ with m_A the gauge boson mass and T the supernova temperature, the production rate P_A is proportional to

$$P_A \sim g_b^2 \times [R(T - m_A)]^n \times \frac{1}{T^2} \simeq \frac{T^{n-2}}{M_s^n}, \quad (1.6)$$

where the factor $[R(T - m_A)]^n$ counts the number of Kaluza–Klein (KK) excitations of the $U(1)_b$ gauge boson with mass less than T . This rate can be compared with the corresponding graviton production

$$P_G \sim \frac{1}{M_P^2} \times (RT)^n \simeq \frac{T^n}{M_s^{n+2}}, \quad (1.7)$$

showing that for $n = 2$ (sub)millimeter extra dimensions, it is unacceptably large, unless the bulk gauge boson acquires a mass $m_A \gtrsim 10$ MeV.

The paper is organized in seven sections, of which this introduction is Section 1. In Section 2, we perform a systematic search for models with four sets of branes corresponding to the gauge group $U(3)_c \times U(2)_L \times U(1)_1 \times U(1)_b$ with the minimal standard model fermion spectrum and a Higgs sector that generates masses for all quarks and leptons of the heaviest generation. We identify the hypercharge $U(1)_Y$ combination and in Section 3 we perform a renormalization group analysis of gauge couplings to identify models with low string scale, where the $U(1)_1$ is on top of either the color or the weak branes. In Section 4, we select four models with string scale in the TeV region, possessing in addition baryon and lepton number conservation, and we describe their main phenomenological features.⁴ They all contain two Higgs doublets that can provide tree-level masses to all fermions. Moreover, apart from the hypercharge, all other Abelian

⁴ Orientifold models with baryon and lepton number conservation were also constructed in Ref. [9].

factors are broken by mixed gauge and gravitational anomalies and become massive at the string scale. In Section 5, we compute the tree-level Yukawa couplings of the two higgses to the fermions of the heaviest generation and study predictions for mass relations. In Section 6, we introduce one right-handed neutrino in the bulk and study the generation of neutrino masses and neutrino oscillations. Finally, Section 7 contains our summary and conclusions.

2. Model search

As shown in [1], the minimal D-brane configuration that can successfully accommodate the Standard Model (SM) consists of three sets of branes with gauge symmetry $U(3)_c \times U(2)_L \times U(1)_1$. The first set contains three coincident branes (“color” branes). An open string with one end attached to this set transforms as an $SU(3)_c$ triplet (or anti-triplet), but also carries an additional $U(1)_c$ quantum number which can be identified with the (gauged) baryon number. Similarly, $U(2)_L$ is realized by a set of two coincident branes (“weak” branes) and open strings attached to them from the one end are $SU(2)_L$ doublets characterized by an additional $U(1)_L$ quantum number, the (gauged) weak “doublet” number. Moreover, consistency of the SM embedding requires the presence of an additional $U(1)_1$ factor, generated by a single brane. This is needed for several reasons: TeV scale unification, baryon number conservation, and mass generation for all quarks and leptons of the heaviest generation. The hypercharge is then a linear combination of the three Abelian factors, $Y = k_3 Q_c + k_2 Q_L + k_1 Q_1$, where Q_c, Q_L, Q_1 are the charges under $U(1)_c, U(1)_L, U(1)_1$, respectively. It turns out [1] that there exist four possible “viable” models that reproduce the weak mixing angle all low energies. They correspond to $k_3 = \frac{2}{3}$ ($k_3 = -\frac{1}{3}$), $k_2 = \pm \frac{1}{2}$, $k_1 = 1$ and require the Abelian brane $U(1)_1$ to be on top of the color (weak) branes, so that $g_3 = g_1$ ($g_2 = g_1$).

In all the above brane configurations there exist states (e.g., the $SU(2)_L$ singlet anti-quarks) which correspond to open strings with only one of their ends attached to one of the three sets of D-branes. The other end is in the bulk, and requires the existence of some additional branes extended in the bulk, carrying extra quantum numbers. In this work, we consider a minimal extension of the models considered in [1] by introducing one additional D-brane in the bulk giving rise to an extra Abelian gauge factor $U(1)_b$. As we will see later, the requirement of baryon and lepton number conservation leads to four possible models that we are going to study in the next section. However, in this section, we do not impose this constraint and we systematically explore the possibility of reproducing the SM spectrum, together with possibly additional Higgs scalars, as open strings stretched between any two of the four sets of branes. The extension of the Higgs sector is required for the realization of the electroweak symmetry breaking and mass generation for all fermions of at least one (the heaviest) generation.

Thus, the total gauge group is

$$\begin{aligned} G &= U(3)_c \times U(2)_L \times U(1)_1 \times U(1)_b \\ &= SU(3)_c \times U(1)_c \times SU(2)_L \times U(1)_L \times U(1)_1 \times U(1)_b \end{aligned} \quad (2.1)$$

Table 1

SM particles with their generic charges under the Abelian part of the gauge group $U(3)_c \times U(2)_L \times U(1)_1 \times U(1)_b$

Particle	$U(1)_c$	$U(1)_L$	$U(1)_1$	$U(1)_b$
$Q(\mathbf{3}, \mathbf{2}, \frac{1}{6})$	+1	w	0	0
$u^c(\bar{\mathbf{3}}, \mathbf{1}, -\frac{2}{3})$	-1	0	a_1	a_2
$d^c(\bar{\mathbf{3}}, \mathbf{1}, +\frac{1}{3})$	-1	0	b_1	b_2
$L(\mathbf{1}, \mathbf{2}, -\frac{1}{2})$	0	+1	c_1	c_2
$e^c(\mathbf{1}, \mathbf{1}, +1)$	0	d_L	d_1	d_2

and contains four Abelian factors. The assignment of the SM particles is partially fixed from its non-Abelian structure. The quark doublet Q corresponds to an open string with one end on the color and the other on the weak set of branes. The anti-quarks u^c, d^c must have one of their ends attached to the color branes. The lepton doublet and possible Higgs doublets must have one end on the weak branes. However, there is a freedom related to the Abelian structure, since the hypercharge can arise as a linear combination of all four Abelian factors. In a generic model, the Abelian charges can be expressed without loss of generality in terms of ten parameters displayed in Table 1.

In a convenient parametrization, normalizing the $U(N) \sim SU(N) \times U(1)$ generators as $\text{Tr} T^a T^b = \delta^{ab}/2$, and measuring the corresponding $U(1)$ charges with respect to the coupling $g/\sqrt{2N}$, the ten parameters are integers: $a_{1,2}, b_{1,2}, c_{1,2}, d_2 = 0, \pm 1, d_1 = 0, \pm 1, \pm 2, d_L = 0, \pm 2, w = \pm 1$ satisfying

$$\sum_{i=1,2} |a_i| = \sum_{i=1,2} |b_i| = \sum_{i=1,2} |c_i| = 1, \quad \sum_{i=1,2,L} |d_i| = 2. \quad (2.2)$$

The first three constraints in (2.2) correspond to the requirement that the u^c and d^c anti-quarks, as well as the lepton doublet, must come from open strings with one end attached to one of the Abelian D-brane sets. The fourth constraint forces the positron e^c open string to be stretched either between the two Abelian branes, or to have both ends attached to the Abelian $U(1)_1$ brane, or to the weak set of branes. In the latter case, it has $U(1)_L$ charge ± 2 and is an $SU(2)_L$ singlet arising from the anti-symmetric product of two doublets. The parameter w in Table 1 refers to the $U(1)_L$ charges of the quark-doublets, that we can choose to be ± 1 , since doublets are equivalent with anti-doublets. Note that a priori one might also consider the case in which one of the u^c and d^c anti-quarks arises as a string with both ends on the color branes ($\mathbf{3} \times \mathbf{3} = \bar{\mathbf{3}} + \mathbf{6}$), so that its $U(1)_c$ charges would be ± 2 . This, however, would invalidate the identification of $U(1)_c$ with the baryon number and forbid the presence of quark mass terms, since one of the combinations Qu^c and Qd^c would not be neutral under $U(1)_c$. Hence, this case will not be explored.

The hypercharge can in general be a linear combination of all four Abelian group factors. However, we restrict ourselves to models in which the bulk $U(1)_b$ does not contribute to the hypercharge, in order to avoid an unrealistically small gauge coupling. Hence,

$$Y = k_3 Q_c + k_2 Q_L + k_1 Q_1. \quad (2.3)$$

The correct assignments for SM particles are reproduced, provided

$$\begin{aligned}
 k_3 + k_2 w &= \frac{1}{6}, \\
 -k_3 + a_1 k_1 &= -\frac{2}{3}, \\
 -k_3 + b_1 k_1 &= \frac{1}{3}, \\
 k_2 + c_1 k_1 &= -\frac{1}{2}, \\
 k_2 d_L + d_1 k_1 &= 1.
 \end{aligned} \tag{2.4}$$

Notice that the second and third of the above equations imply that $k_1 \neq 0$.

The next step, after assigning the correct hypercharge to the SM particles, is to check for the existence of candidate fermion mass terms. Here, we discuss only the question of masses for one generation (the heaviest) and we do not address the general problem of flavor. To lowest order, the mass terms are of the form $Qd^c H_d^\dagger$, $Qu^c H_u$ and $Le^c H_e^\dagger$ where H_d , H_u , H_e are scalar Higgs doublets with appropriate charges. In a generic model, there are four different candidate Higgs scalar doublets (and their conjugates) H_1, \dots, H_4 , with $U(1)_L \times U(1)_1 \times U(1)_b$ charges:

$$\{H_1, H_2, H_3, H_4\} = \{(1, 1, 0), (1, 0, 1), (1, -1, 0), (1, 0, -1)\}. \tag{2.5}$$

It is easy to show that for any hypercharge embedding of the form (2.3) with $k_1 \neq 0$, there are at most three of the above Higgs doublets that have the correct hypercharge. Depending on the parameters of the model, they can be reduced to two. For the generic charge assignments of Table 1, the required Higgs charges are

$$\begin{aligned}
 H_u &= (\mathbf{1}, \mathbf{2}, 0, -w, -a_1, -a_2), \\
 H_d &= (\mathbf{1}, \mathbf{2}, 0, +w, +b_1, +b_2), \\
 H_e &= (\mathbf{1}, \mathbf{2}, 0, 1 + d_L, c_1 + d_1, c_2 + d_2).
 \end{aligned} \tag{2.6}$$

Provided the constraints (2.2) are satisfied, both H_u and H_d have the right charges of (2.5) and correspond to strings stretched between the weak and one of the Abelian branes. Thus, (2.2) guarantees the existence of tree-level quark masses. On the other hand, the existence of H_e depends on the particular choice of parameters, e.g., for $c_1 + d_1 = 2$, H_e does not exist and a tree-level lepton mass term ($Le^c H^\dagger$) is forbidden. The generic constraint that guarantees tree-level lepton masses is

$$\sum_{i=1,2} |c_i + d_i| = |1 + d_L| = 1. \tag{2.7}$$

Given the smallness of the lepton mass compared to the masses of the quarks, of the same generation, it would be reasonable to examine also the possibility that the lepton mass is generated by a higher order term. The next order candidate lepton mass term is of dimension six, proportional to $\frac{1}{M_s^2} Le^c H^\dagger H^\dagger H$. The constraint in this case is more complicated and the method we are going to use is the following: for each configuration

that satisfies all other constraints except (2.7), we derive explicitly the candidate Higgs doublets and check the existence of possible fifth order mass terms.⁵

The hypercharge constraints (2.4) can be easily solved. They require $a_1 \neq b_1$ and

$$k_3 = \frac{a_1 + 2b_1}{3(b_1 - a_1)}, \quad (2.8)$$

$$k_2 = -\frac{(a_1 + b_1)}{2(b_1 - a_1)w}, \quad (2.9)$$

$$k_1 = \frac{1}{b_1 - a_1}, \quad (2.10)$$

$$c_1 = -\frac{b_1 - a_1}{2} + \frac{(a_1 + b_1)}{2w}, \quad (2.11)$$

$$d_1 = b_1 - a_1 + \frac{(a_1 + b_1)d_L}{2w}. \quad (2.12)$$

The allowed values of (a_1, b_1) are $\{(-1, 0), (-1, 1), (0, -1), (0, 1), (1, -1), (1, 0)\}$. However, we notice that the solutions with parameters $(a_1, b_1, c_1, d_1, k_1)$ and $(-a_1, -b_1, -c_1, -d_1, -k_1)$ are equivalent, since they correspond to a global change of sign $Q_1 \rightarrow -Q_1$. Thus, it is sufficient to search for solutions with $(a_1, b_1) \in \{(-1, 0), (-1, 1), (0, 1)\}$. Solving for these choices, we get three allowed hypercharge embeddings:

$$(i) \quad a_1 = -1, b_1 = 1: \quad Y = \frac{1}{6}Q_c + \frac{1}{2}Q_1, \quad (2.13)$$

$$(ii) \quad a_1 = -1, b_1 = 0: \quad Y = -\frac{1}{3}Q_c + \frac{w}{2}Q_L + Q_1, \quad (2.14)$$

$$(iii) \quad a_1 = 0, b_1 = 1: \quad Y = \frac{2}{3}Q_c - \frac{w}{2}Q_L + Q_1. \quad (2.15)$$

Case (i) leads to $c_1 = -1, c_2 = 0, d_1 = 2, d_1 = d_L = 0$. This is a special solution where the $U(1)_b$ brane decouples from the model since no SM particles are attached to it. It satisfies (2.7) and thus leads to tree level lepton masses. The solution exists for both $w = \pm 1$, as the value of w does not play an important role when $k_2 = 0$. In case (ii), we have $c_1 = -(1+w)/2, d_L = 0, d_1 = 1$ or $c_1 = (1+w)/2, d_L = 2w, d_1 = d_2 = 0$, while case (iii) leads to $c_1 = (w-1)/2, d_L = 0, d_1 = 1$ or $c_1 = (1+w)/2, d_L = 2w, d_1 = d_2 = 0$.

Combining the above three cases with the constraints (2.2) and (2.7), we get 9 distinct configurations with tree-level quark and lepton masses, displayed in the upper part of Table 2. Relaxing the constraint (2.7) with the requirement that lepton masses arise through dimension six effective operators, leads to 6 more distinct models corresponding to the cases 10–15 of Table 2. In deriving these configurations, we have eliminated all models connected to the ones above by the global charge redefinition $Q_b \rightarrow -Q_b$.

As we mentioned before, in all the above configurations, we can define the baryon number B as

$$B = \frac{1}{3}Q_c. \quad (2.16)$$

⁵ Here, we check only the conservation of all gauge quantum numbers. In the string context, there may be additional selection rules for the non-vanishing of the corresponding couplings that are model dependent.

Table 2

Distinct models with lepton masses generated either at tree level $Le^c H^\dagger$ (cases 1–9), or by dimension six effective operators $\sim Le^c H^\dagger \langle H^\dagger H \rangle / M^2$ (cases 10–15). We also display the lepton number combination L (when it exists) and the number of Higgs doublets n_h , needed to generate quark and lepton masses

	a_1	a_2	b_1	b_2	c_1	c_2	d_1	d_2	d_L	w	Y	L	n_h
1	-1	0	1	0	-1	0	2	0	0	1	$\frac{1}{6}Q_c + \frac{1}{2}Q_1$	-	2
2	-1	0	0	-1	0	-1	1	1	0	-1	$-\frac{1}{3}Q_c - \frac{1}{2}Q_L + Q_1$	$\frac{1}{2}Q_c + \frac{1}{2}Q_L - \frac{1}{2}Q_1 - \frac{1}{2}Q_b$	2
3	-1	0	0	-1	-1	0	1	1	0	1	$-\frac{1}{3}Q_c + \frac{1}{2}Q_L + Q_1$	-	3
4	0	1	1	0	0	-1	1	1	0	1	$\frac{2}{3}Q_c - \frac{1}{2}Q_L + Q_1$	$-\frac{1}{2}Q_c + \frac{1}{2}Q_L - \frac{1}{2}Q_1 - \frac{1}{2}Q_b$	2
5	0	1	1	0	-1	0	1	1	0	-1	$\frac{2}{3}Q_c + \frac{1}{2}Q_L + Q_1$	-	3
6	-1	0	0	-1	0	-1	0	0	-2	-1	$-\frac{1}{3}Q_c - \frac{1}{2}Q_L + Q_1$	$\frac{1}{2}Q_c + \frac{1}{2}Q_L - \frac{1}{2}Q_1 - \frac{1}{2}Q_b$	2
7	-1	0	0	1	0	-1	0	0	-2	-1	$-\frac{1}{3}Q_c - \frac{1}{2}Q_L + Q_1$	-	3
8	0	1	1	0	0	1	0	0	-2	1	$\frac{2}{3}Q_c - \frac{1}{2}Q_L + Q_1$	-	3
9	0	1	1	0	0	-1	0	0	-2	1	$\frac{2}{3}Q_c - \frac{1}{2}Q_L + Q_1$	$-\frac{1}{2}Q_c + \frac{1}{2}Q_L - \frac{1}{2}Q_1 - \frac{1}{2}Q_b$	2
10	-1	0	0	1	-1	0	0	0	2	1	$-\frac{1}{3}Q_c + \frac{1}{2}Q_L + Q_1$	-	3
11	0	1	1	0	-1	0	0	0	2	-1	$\frac{2}{3}Q_c + \frac{1}{2}Q_L + Q_1$	-	3
12	-1	0	0	1	0	1	1	1	0	-1	$-\frac{1}{3}Q_c - \frac{1}{2}Q_L + Q_1$	-	3
13	-1	0	0	-1	0	1	1	1	0	-1	$-\frac{1}{3}Q_c - \frac{1}{2}Q_L + Q_1$	-	3
14	0	1	1	0	0	1	1	1	0	1	$\frac{2}{3}Q_c - \frac{1}{2}Q_L + Q_1$	-	3
15	0	1	1	0	0	-1	1	-1	0	1	$\frac{2}{3}Q_c - \frac{1}{2}Q_L + Q_1$	-	3

As we will argue below, $U(1)_c$ gauge invariance is broken by anomalies to a global symmetry, implying baryon number conservation in type I string perturbation theory. Since lepton number is also conserved at present energies, we can further examine which of the above models possess also the lepton number L as a symmetry. In general, L can also be expressed as a linear combination of all Abelian factors,

$$L = \sum_{i=c,L,1,b} p_i Q_i \quad (2.17)$$

that satisfies

$$\begin{aligned} p_c + p_L w &= 0, \\ -p_c + a_1 p_1 + a_2 p_b &= 0, \\ -p_c + b_1 p_1 + b_2 p_b &= 0, \\ p_L + c_1 p_1 + c_2 p_b &= 1, \\ d_L p_L + d_1 p_1 + d_2 p_b &= -1. \end{aligned} \quad (2.18)$$

Inspection of (2.18), in conjunction with (2.4) that requires $a_1 \neq b_1$, implies that lepton number can only be defined for $p_b \neq 0$, i.e., only in the presence of the bulk $U(1)_b$. This is of course expected, since the models without $U(1)_b$ have no lepton number [1]. Solving explicitly (2.18) for each one of the cases of Table 2, we find that only four models, namely 2, 4, 6, 9, incorporate the lepton number as a (gauged) Abelian symmetry. Its precise definition for each of these models is also presented in Table 2.

3. The weak angle and the string scale

We now come to the determination of the string scale consistent with the low energy SM data. Following the hypercharge definition (2.3), the low energy data depend on the couplings g_3 , g_2 and g_1 of the three brane sets $U(3)_c$, $U(2)_L$ and $U(1)_1$. These couplings are in principle independent, but, as already explained in the introduction, in order to lower the string scale we have to consider configurations where the $U(1)_1$ brane is on top of either the $U(3)_c$ or the $U(2)_L$ stacks. Hence, we have two possible coupling relations at the string scale

$$(i): g_3 = g_1 \quad \text{or} \quad (ii): g_2 = g_1. \quad (3.1)$$

In our normalizations, the hypercharge coupling g_Y at the string scale is expressed as

$$\frac{1}{g_Y^2} = \frac{6k_3^2}{g_3^2} + \frac{4k_2^2}{g_2^2} + \frac{2k_1^2}{g_1^2}. \quad (3.2)$$

Following the one loop coupling evolution ($\alpha_i = g_i^2/4\pi$),

$$\frac{1}{\alpha_i(M_s)} = \frac{1}{\alpha_i(M_Z)} + \frac{b_i}{4\pi} \ln \frac{\Delta^1 M_s}{M_Z}, \quad (3.3)$$

where $b_3 = -7$, $b_2 = -10/3 + n_h/6$, $b_Y = 20/3 + n_h/6$ and n_h is the number of scalar Higgs doublets. The constant Δ^1 corresponds to a model independent piece of the type I string thresholds, entering in the identification of the string scale with the ultraviolet cutoff of the effective field theory. Its value was computed in Ref. [12] to be $\Delta^1 = 1/\sqrt{\pi e^\gamma} \simeq 0.4$, where γ is the Euler's constant. When the string scale is very high compared to present energies, this represents a small correction compared to the dominant logarithmic contribution coming from the renormalization group evolution. On the other hand, when the string scale is low, such a correction becomes important, as it effectively changes the string scale by roughly a factor of two, and should be taken with caution since it is of the same order with the (unknown) model dependent part of threshold corrections. Consequently, we will leave Δ^1 as a parameter and discuss its possible effects on our results case by case.

Solving the one-loop renormalization group equations (RGE) for the coupling evolution, the values of the weak mixing angle $\sin^2 \theta_W$ and of the strong coupling a_3 at the Z -mass M_Z are related to the couplings at the string scale:

$$\begin{aligned} \sin^2 \theta_W(M_Z) = & \frac{1}{1+k_Y} + \frac{\alpha_{em}(M_Z)}{2\pi} \frac{(k_Y b_2 - b_Y)}{(1+k_Y)} \ln \frac{\Delta^1 M_s}{M_Z} \\ & + \frac{\alpha_{em}(M_Z)}{1+k_Y} \left[6k_3^2 \left(\frac{1}{\alpha_L(M_s)} - \frac{1}{\alpha_3(M_s)} \right) \right. \\ & \left. + 2k_1^2 \left(\frac{1}{\alpha_L(M_s)} - \frac{1}{\alpha_1(M_s)} \right) \right], \end{aligned} \tag{3.4}$$

$$\begin{aligned} \frac{1}{a_3(M_Z)} = & \frac{1}{\alpha_{em}(M_Z)} \frac{1}{1+k_Y} - \frac{1}{2\pi} \frac{b_2 + b_Y - b_3(1+k_Y)}{1+k_Y} \log \frac{\Delta^1 M_s}{M_Z} \\ & + \frac{1}{1+k_Y} \left[(4k_2^2 + 1) \left(\frac{1}{\alpha_L(M_s)} - \frac{1}{\alpha_3(M_s)} \right) \right. \\ & \left. - 2k_1^2 \left(\frac{1}{\alpha_L(M_s)} - \frac{1}{\alpha_1(M_s)} \right) \right], \end{aligned} \tag{3.5}$$

where $k_Y = 6k_3^2 + 4k_2^2 + 2k_1^2$ and α_{em} is the electromagnetic coupling.

Given a coupling relation of (3.1), we can use Eqs. (3.4) and (3.5) to determine the string scale M_s that correctly reproduces the low energy data. Clearly, the solution depends on $|k_3|$, $|k_2|$ and $|k_1|$. According to our previous analysis, there are three classes of models, which correspond to the three possible hypercharge embeddings (2.13), (2.14) and (2.15):

$$\begin{aligned} \text{(i):} \quad & |k_3| = \frac{1}{6}, \quad |k_2| = 0, \quad |k_1| = \frac{1}{2}, \\ \text{(ii):} \quad & |k_3| = \frac{1}{3}, \quad |k_2| = \frac{1}{2}, \quad |k_1| = 1, \\ \text{(iii):} \quad & |k_3| = \frac{2}{3}, \quad |k_2| = \frac{1}{2}, \quad |k_1| = 1. \end{aligned} \tag{3.6}$$

Using (3.4) and (3.5), for each of the embeddings (3.6) and the unification conditions (3.1), we computed the corresponding string ‘‘unification’’ scale $M_U \equiv \Delta^1 M_s$. In our calculation

Table 3

The string unification scale M_U and the two independent gauge couplings for the two possible brane configurations and the various hypercharge embeddings

	$ k_3 $	$ k_2 $	$ k_1 $	M_U (TeV)	$g_2(M_U)/g_3(M_U)$	$g_2(M_U)g_3(M_U)$
$g_1 = g_3$	$\frac{1}{6}$	0	$\frac{1}{2}$	4.6×10^{20}	1.1	0.21
	$\frac{1}{3}$	$\frac{1}{2}$	1	2.4×10^3	0.76	0.48
	$\frac{2}{3}$	$\frac{1}{2}$	1	7.2	0.65	0.61
$g_1 = g_2$	$\frac{1}{6}$	0	$\frac{1}{2}$	1.5×10^{22}	1.1	0.26
	$\frac{1}{3}$	$\frac{1}{2}$	1	0.32	0.57	0.73
	$\frac{2}{3}$	$\frac{1}{2}$	1	–	–	–

we have used the following values for the low energy quantities $a_3(M_Z) = 0.119$, $\sin^2 \theta_W = 0.231$, $a_{em}(M_Z) = 1/127.934$. The results are presented in Table 3.

In the above calculations we have assumed that the number of doublets n_h is the minimum $n_h = 2$ required by the model. Of course, one can consider models with more doublets which can be for instance replicas of these two. It would be thus interesting to examine the dependence of the above results on the number of doublets. To this end we can extract analytic formulas regarding the unification scale M_U . For the case $g_1 = g_3$, taking for simplicity $k_1 = 1$ and $k_L = \pm \frac{1}{2}$, we find

$$\frac{3(4 + 7k_3^2)}{\pi} \log \frac{M_U}{M_Z} = \frac{1}{\alpha_{em}(M_Z)} (1 - 2 \sin^2 \theta_W(M_Z)) - 2(1 + 3k_3^2) \frac{1}{\alpha_3(M_Z)} \quad (3.7)$$

which implies that at the one-loop M_U is independent of the number of doublets. Similarly, for $g_1 = g_2$ and $k_1 = 1$, $k_L = \pm \frac{1}{2}$, we have

$$\frac{50 + 126k_3^2 - n_h}{6\pi} \log \frac{M_U}{M_Z} = \frac{1}{\alpha_{em}(M_Z)} (1 - 4 \sin^2 \theta_W(M_Z)) - 6k_3^2 \frac{1}{\alpha_3(M_Z)}, \quad (3.8)$$

where we find a very weak dependence. Obviously, the number of doublets affects the value of the weak gauge coupling at M_s and thus the volume of the bulk through (1.3).

4. The models

So far, we have classified all possible $U(3)_c \times U(2)_L \times U(1)_1 \times U(1)_b$ brane models that can successfully accommodate the SM spectrum. The quantum numbers of each model as well as the hypercharge embedding are summarized in Table 2. Furthermore, compatibility with type I string theory with string scale in the TeV region, requires the bulk to be two-dimensional of (sub)millimeter size, and leads to two possible configurations: place the $U(1)_1$ brane on top of the weak $U(2)_L$ stack of branes or on top of the color $U(3)_c$ branes. These impose two different brane coupling relations at the string (unification) scale: $g_1 = g_2$ or $g_1 = g_3$, respectively. For every model, using the hypercharge embedding of Table 2, the one loop gauge coupling evolution and one of the above brane coupling

conditions, we can determine the unification (string) scale that reproduces the weak angle at low energies. The results are summarized in Table 3.

According to the results of Section 2, there are three distinct hypercharge embeddings that correspond to $(|k_3|, |k_2|, |k_1|) = \{(1/6, 0, 1/2), (1/3, 1/2, 1), (2/3, 1/2, 1)\}$. Since we wish to restrict ourselves to models in which supersymmetry is broken at the string scale (M_s), we would like M_s to be low, at the TeV scale, to protect the mass hierarchy. Thus, model 1 of Table 2, with hypercharge embedding $(1/6, 0, 1/2)$, is rejected for both $U(1)_1$ brane arrangements, since the resulting string scale is too high. Furthermore, models with hypercharge embedding $(1/3, 1/2, 1)$ lead to $M_s \sim 10^3$ TeV for $g_1 = g_3$. This scale, although much lower than the traditional GUT scale, is rather high for the stabilization of hierarchy. On the contrary, for $g_1 = g_2$, we find $M_s \sim \mathcal{O}(1)$ TeV (when the universal threshold correction Δ^1 is taken into account) that lies at the edge of the present experimental limits. The third embedding $(2/3, 1/2, 1)$ reproduces successfully the low energy data only for $g_1 = g_3$ and a string scale $M_s \sim \mathcal{O}(10)$ TeV.

In all configurations of Table 2, the baryon number appears as a gauged Abelian symmetry. This symmetry is broken due to mixed gauge and gravitational anomalies leaving behind a global symmetry. Baryon number conservation is essential for low string scale models, since one needs to eliminate effective operators to very high accuracy in order to avoid fast proton decay, starting with dimension six operators of the form $QQQL$ which are not sufficiently suppressed [13]. In addition to baryon number, one should also assure that the lepton number is a good symmetry of the low energy theory. Lepton number conservation is also essential for preservation of acceptable neutrino masses, as it forbids for instance the presence of the dimension 5 operator $LLHH$. Such an operator would lead to large Majorana neutrino masses, of the order of a few GeV, in models where the string scale, typically a few TeV, is too low for the operation of an effective sea-saw mechanism. Hence, we shall be interested only in models in which the lepton number is a good symmetry. Indeed, as seen in Table 2, only in four models, namely 2, 4, 6 and 9, lepton number appears as a (gauged) Abelian symmetry. Being anomalous, this symmetry will be broken, but lepton number will survive as a global symmetry of the effective theory.

In fact, these four models can be derived in a straightforward way by simple considerations of the quantum numbers. The quark doublet Q is fixed by non-Abelian gauge symmetries, while existence of baryon number implies that the anti-quarks u^c, d^c correspond to strings stretched between the color branes and one each of the Abelian branes $U(1)_1$ and $U(1)_b$. Thus, one has two possibilities leading to models that we call A (d^c has one end in the bulk) and B (u^c sees the bulk). Existence of lepton number fixes the lepton doublet as a string stretched between the weak branes and the $U(1)_b$ brane, while for each of the models A and B there are two possibilities for the anti-lepton e^c to emerge as a string stretched between the two Abelian branes, or to have both ends on the weak branes. Thus, we obtain two additional models that we call A' and B'. As it can also be seen in the table, all these models have tree-level quark and lepton masses and make use of only two Higgs doublets. They also require low energy string scale for some of the brane coupling conditions. We now proceed to a detailed study of these four models and to an analysis of their main phenomenological characteristics.

Notice from Table 3 that in both classes of models A and B, the coupling constant ratio is $g_2/g_3 \simeq 0.6$ at the string scale, implying through the relations of Section 1 that

at least one of the internal compact dimensions along the world-volume of the weak set of branes must be larger than the string length, by at least a factor of two (in the case of two large dimensions, or by a factor of four in the case of one). The relevant experimental signal would be the production of Kaluza–Klein excitations for the W^\pm bosons and the other mediators of the electroweak interactions but not of gluons, providing one of the first indications of new physics [14].

4.1. Models A and A'

We consider here the models 2 and 6 of Table 2, hereafter referred as models A and A', respectively. They are characterized by the common hypercharge embedding

$$Y = -\frac{1}{3}Q_c - \frac{1}{2}Q_L + Q_1 \tag{4.1}$$

but they differ slightly in their spectra. The spectrum of model A is

- $Q(\mathbf{3}, \mathbf{2}, +1, -1, 0, 0),$
- $u^c(\bar{\mathbf{3}}, \mathbf{1}, -1, 0, -1, 0),$
- $d^c(\bar{\mathbf{3}}, \mathbf{1}, -1, 0, 0, -1),$
- $L(\mathbf{1}, \mathbf{2}, 0, +1, 0, -1),$
- $e^c(\mathbf{1}, \mathbf{1}, 0, 0, +1, +1),$
- $H_u(\mathbf{1}, \mathbf{2}, 0, +1, +1, 0),$
- $H_d(\mathbf{1}, \mathbf{2}, 0, -1, 0, -1),$

while in model A' the right-handed electron e^c is replaced by an open string with both ends on the weak brane stack, and thus $e^c = (\mathbf{1}, \mathbf{1}, 0, -2, 0, 0)$. The two models are presented pictorially in Fig. 1.

Apart from the hypercharge combination (4.1) all remaining Abelian factors are anomalous. Indeed, for every Abelian generator $Q_I, I = (c, L, 1, b)$, we can calculate the mixed gauge anomaly $K_{IJ} \equiv \text{Tr } Q_I T_J^2$ with $J = SU(3), SU(2), Y$, and gravitational

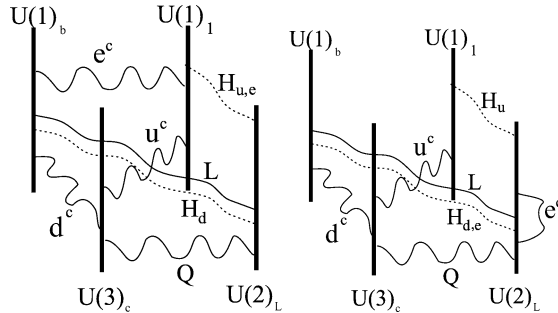


Fig. 1. Pictorial representation of models A, A'.

anomaly $K_{I4} \equiv \text{Tr } Q_I$ for both models A and A':

$$K^{(A)} = \begin{pmatrix} 0 & -1 & -\frac{1}{2} & -\frac{1}{2} \\ \frac{3}{2} & -1 & 0 & -\frac{1}{2} \\ -\frac{3}{2} & \frac{1}{3} & -\frac{1}{3} & \frac{1}{6} \\ 0 & -4 & -2 & -4 \end{pmatrix}, \quad K^{(A')} = \begin{pmatrix} 0 & -1 & -\frac{1}{2} & -\frac{1}{2} \\ \frac{3}{2} & -1 & 0 & -\frac{1}{2} \\ -\frac{3}{2} & -\frac{5}{3} & -\frac{4}{3} & -\frac{5}{6} \\ 0 & -6 & -3 & -5 \end{pmatrix}. \quad (4.2)$$

It is easy to check that the matrices KK^T for both models have only one zero eigenvalue corresponding to the hypercharge combination (4.1) and three non-vanishing ones corresponding to the orthogonal $U(1)$ anomalous combinations. In the context of type I string theory, these anomalies are canceled by a generalized Green–Schwarz mechanism which makes use of three axions that are shifted under the corresponding $U(1)$ anomalous gauge transformations [15]. As a result, the three extra gauge bosons become massive, leaving behind the corresponding global symmetries unbroken in perturbation theory [16]. The three extra $U(1)$'s can be expressed in terms of known SM symmetries:

$$\begin{aligned} \text{Baryon number: } B &= \frac{1}{3}Q_c, \\ \text{Lepton number: } L &= \frac{1}{2}(Q_c + Q_L - Q_1 - Q_b), \\ \text{Peccei–Quinn: } Q_{\text{PQ}} &= -\frac{1}{2}(Q_c - Q_L - 3Q_1 - 3Q_b). \end{aligned} \quad (4.3)$$

Thus, our effective SM inherits baryon and lepton number as well as Peccei–Quinn (PQ) global symmetries from the anomaly cancellation mechanism. Note however that PQ is the original Peccei–Quinn symmetry only in model A', such that all fermions have charges +1, while H_u and H_d have charges -2 and $+2$, respectively. In model A, the global PQ symmetry defined in (4.3) is similar but with lepton charge +3. The reason is that in model A the fermion-Higgs Yukawa couplings are different, and leptons get masses from H_u and not from H_d .

The general one-loop string computation of the masses of anomalous $U(1)$ gauge bosons, as well as their localization properties in the internal compactified space, was performed recently for generic orientifold vacua [17]. It was shown that orbifold sectors preserving $N = 1$ supersymmetry yield four-dimensional (4d) contributions, localized in the whole six-dimensional (6d) internal space, while $N = 2$ supersymmetric sectors give 6d contributions localized only in four internal dimensions. The later are related to 6d anomalies. Thus, even $U(1)$ s which are apparently anomaly free may acquire non-zero masses at the one-loop level, as a consequence of 6d anomalies. These results have the following implications in our case:

- (1) The two $U(1)$ combinations, orthogonal to the hypercharge and localized on the strong and weak D-brane sets, acquire in general masses of the order of the string scale from contributions of $N = 1$ sectors, in agreement with effective field theory expectations based on 4d anomalies.
- (2) Such contributions are not sufficient though to make heavy the third $U(1)$ propagating in the bulk, since the resulting mass terms are localized and suppressed by the

volume of the bulk. In order to give string scale mass, one needs instead $N = 2$ contributions associated to 6d anomalies along the two large bulk directions. In our models such contributions are indeed in general present and arise from mixed 6d gauge-gravitational anomalies of two different sources: (i) the generic presence of a neutral 6d Weyl fermion on the bulk brane which coincides either with the $U(1)_b$ gaugino (in the supersymmetric case) or the goldstino of the non-linearly realized supersymmetry (in the brane SUSY breaking case [7]); (ii) the contribution of the right-handed neutrino which arises from a six-dimensional Weyl spinor. As a result, the third Abelian gauge field $U(1)_b$ acquires also a mass of the order of the string scale, although its gauge coupling is tiny due to the volume suppression (see Eq. (1.5)).

- (3) Special care is needed to guarantee that the hypercharge remains massless despite the fact that it is anomaly free, along the lines of Ref. [17].

The presence of massive gauge bosons associated to anomalous Abelian gauge symmetries is generic. Their mass is given by $M_A^2 \sim g_s M_s^2$, up to a numerical model dependent factor and is somewhat smaller than the string scale. When the latter is low, they can affect low energy measurable data, such as $g - 2$ for leptons [18] and the ρ -parameter [19], leading to additional bounds on the string scale.

Note that the global PQ symmetry leftover from $U(1)_b$ is spontaneously broken by the Higgs expectation value giving rise to an unwanted electroweak axion. A possible way out was suggested in Ref. [1], using an appropriate departure away from the orientifold point.

A plausible extension of the model is the introduction of a right-handed neutrino in the bulk. A natural candidate state would be an open string ending on the $U(1)_b$ brane. Its charge is then fixed to $+2$ by the requirement of existence of the single possible neutrino mass term $LH_d\nu_R$. The suppression of the brane-bulk couplings due to the wave function of ν_R would thus provide a natural explanation for the smallness of neutrino masses. Note that if the zero mode of this bulk neutrino state is chiral, the anomaly structure of the model changes: $B - L$ becomes anomaly free and as a consequence the associated gauge boson remains in principle massless. However, as we discussed above, this is not in general true because of 6d anomalies [17]. In any case, this problem is absent if we introduce a vector-like bulk neutrino pair

$$\nu_R(\mathbf{1}, \mathbf{1}, 0, 0, 0, +2) + \nu_R^c(\mathbf{1}, \mathbf{1}, 0, 0, 0, -2)$$

that leaves the anomalies (4.2) intact. Note that ν_R^c does not play any role in the subsequent discussion of neutrino masses and oscillations.

Coming to the issue of gauge couplings and the string scale, as already explained we have two different realizations for each model. The first is with $g_1 = g_3$ at M_s that corresponds to a configuration where the $U(1)_1$ brane is placed on top of the color branes. According to Table 3, this leads to an intermediate string scale $M_s \sim 10^6$ GeV, which appears too high to guarantee the stabilization of hierarchy. The second possibility is to take the $U(1)_1$ brane on top of the weak branes, leading to $g_1 = g_2$. The required string scale is now low $M_s \sim \mathcal{O}(500)$ GeV (300–800 GeV, depending on the threshold corrections), and could account for the stability of the hierarchy.

4.2. *Models B and B'*

Another phenomenologically promising pair of models consists of solutions 4 and 9 of Table 2, named hereafter B and B', which corresponds to the hypercharge embedding

$$Y = \frac{2}{3}Q_c - \frac{1}{2}Q_L + Q_1. \tag{4.4}$$

The spectrum is

- $Q(\mathbf{3}, \mathbf{2}, +1, +1, 0, 0),$
- $u^c(\bar{\mathbf{3}}, \mathbf{1}, -1, 0, 0, 1),$
- $d^c(\bar{\mathbf{3}}, \mathbf{1}, -1, 0, 1, 0),$
- $L(\mathbf{1}, \mathbf{2}, 0, +1, 0, -1),$
- $e^c(\mathbf{1}, \mathbf{1}, 0, 0, +1, +1),$
- $H_u(\mathbf{1}, \mathbf{2}, 0, -1, 0, -1),$
- $H_d(\mathbf{1}, \mathbf{2}, 0, +1, +1, 0),$

for model B, while in B' e^c is replaced by $e^c(\mathbf{1}, \mathbf{1}, 0, -2, 0, 0)$. The two models are represented pictorially in Fig. 2. The four Abelian gauge factors are anomalous. Proceeding as in the analysis (4.2) of models A and A', the mixed gauge and gravitational anomalies are

$$K^{(B)} = \begin{pmatrix} 0 & 1 & \frac{1}{2} & \frac{1}{2} \\ \frac{3}{2} & 2 & 0 & -\frac{1}{2} \\ -\frac{3}{2} & \frac{2}{3} & \frac{4}{3} & \frac{11}{6} \\ 0 & 8 & 4 & 2 \end{pmatrix}, \quad K^{(B')} = \begin{pmatrix} 0 & 1 & \frac{1}{2} & \frac{1}{2} \\ \frac{3}{2} & 2 & 0 & -\frac{1}{2} \\ -\frac{3}{2} & -\frac{4}{3} & \frac{1}{3} & \frac{5}{6} \\ 0 & 6 & 3 & 1 \end{pmatrix}. \tag{4.5}$$

It is easy to see that the only anomaly free combination is the hypercharge (4.4) which survives at low energies. All other Abelian gauge factors are anomalous and will be broken by the generalized Green–Schwarz anomaly cancellation mechanism, leaving behind global symmetries. They can be expressed in terms of the usual SM global symmetries

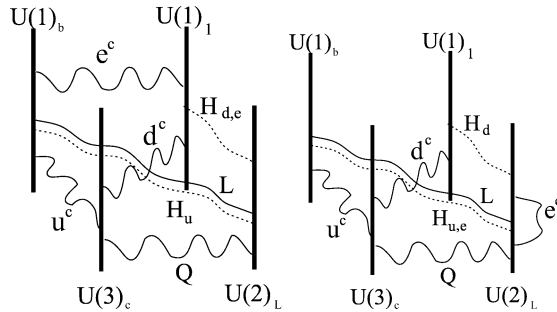


Fig. 2. Pictorial representation of models B and B'.

as the following $U(1)$ combinations:

$$\text{Baryon number: } B = \frac{1}{3} Q_c, \quad (4.6)$$

$$\text{Lepton number: } L = -\frac{1}{2} (Q_c - Q_L + Q_1 + Q_b), \quad (4.7)$$

$$\text{Peccei–Quinn: } Q_{\text{PQ}} = \frac{1}{2} (-Q_c + 3Q_L + Q_1 + Q_b). \quad (4.8)$$

Similarly to the analysis of models A and A', the PQ charges defined above are the traditional ones only for model B. In model B', the lepton charge is -3 , as a result of the Higgs–Yukawa couplings to the fermions (see below). The right handed neutrino can also be accommodated as an open string with both ends on the bulk Abelian brane:

$$\nu_R(\mathbf{1}, \mathbf{1}, 0, 0, 0, +2) + \nu_R^c(\mathbf{1}, \mathbf{1}, 0, 0, 0, -2). \quad (4.9)$$

According to the RGE running results of Table 3, there is only one brane configuration, for the models under discussion, that reproduces the weak mixing angle at low energies. This consists of placing the $U(1)_1$ brane on the top of the color branes, so that $g_1 = g_3$, which leads to $M_s \sim \mathcal{O}(10)$ TeV (7–17 TeV, depending on the threshold corrections).

5. Fermion masses

Although the general question of quark and lepton masses goes beyond the scope of this paper, we would like to make here some comments in the context of our constructions. The Yukawa couplings relevant to fermion masses are constrained by the various $U(1)$ symmetries and can present interesting patterns.

Model A. The relevant Yukawa couplings are

$$M_A = \lambda_u Q u^c H_u + \lambda_d Q d^c H_d^\dagger + \lambda_e L e^c H_u^\dagger + \lambda_\nu L H_d \nu_R. \quad (5.1)$$

Here, charged leptons and up quarks (of the heaviest generation) obtain masses from the same Higgs (H_u).

When all Yukawa couplings arise at the lowest (disk) order, it is easy to check that in the simplest case (absence of discrete selection rules, etc), they satisfy the following relations:

$$\lambda_u = \lambda_e = \sqrt{2} g_2, \quad \lambda_d = \sqrt{2 g_s}, \quad \lambda_\nu = \sqrt{2} g_b. \quad (5.2)$$

The top and bottom quark masses are given by

$$m_t = g_2 v \sin \beta, \quad m_b = \sqrt{g_s} v \cos \beta, \quad (5.3)$$

where $\tan \beta = v_u/v_d$, with v_u and v_d the vacuum expectation values (VEVs) of the two higgses H_u and H_d , respectively, and $v = \sqrt{v_u^2 + v_d^2} = 246$ GeV. Note that in the case where the color branes are identified with D3 branes, one has $\sqrt{g_s} = g_3$, and in any case $g_s \geq g_3^2$. Note also that since the string scale in this model is relatively low, $M_s \lesssim 1$ TeV, there is no much evolution of the low energy couplings from the electroweak to the string scale. Thus, using the known value of the bottom mass $m_b \simeq 4$ GeV, one obtains for the

top quark mass $m_t \simeq 162$ GeV which is less than 5% below its experimental value $m_t^{\text{exp}} = 174.3 \pm 5.1$ GeV. In addition, the Higgs VEV ratio turns out to be large, $\tan \beta \simeq 100$. Note that such a large value is not in principle problematic as in the supersymmetric case, but it can lead to important higher order corrections.

On the other hand the τ -mass is of the same order as the top mass, which is unrealistic. However, there is still the possibility that the lepton Yukawa coupling λ_e vanishes to lowest order due to additional string discrete selection rules, and is generated by a higher-dimensional operator of the form $Le^c(H_u^\dagger H^\dagger H)$ providing the appropriate suppression.⁶

Model A'. The Yukawa couplings here are

$$M_{A'} = \lambda_u Q u^c H_u + \lambda_d Q d^c H_d^\dagger + \lambda_e L e^c H_d^\dagger + \lambda_\nu L H_d \nu_R \quad (5.4)$$

with the same relation for the tree-level couplings as in (5.2). Using the parametrization in (5.3) we see that the relation of m_t to m_b is the same as in model A and the same remarks apply. Since here the lepton and down quark acquire their masses from the same Higgs, one obtains the phenomenologically interesting relation: $m_b/m_\tau = \sqrt{g_s}/g_2 = g_3/g_2$, when strong interactions are on D3-branes. Thus, from Table 3, $m_b/m_\tau \simeq 1.75$ at the (string) unification scale, which is in the upper edge of the experimentally allowed region at the Z-mass, $1.46 \lesssim m_b/m_\tau|_{\text{exp}} \lesssim 1.75$. This relation could replace the successful GUT prediction $m_b = m_\tau$ of the conventional unification framework, in low scale string models. In conclusion model A' seems to be able to generate the required hierarchy of masses for the third generation.

Model B. The relevant trilinear Yukawa couplings are,

$$M_B = \lambda_u Q u^c H_u + \lambda_d Q d^c H_d^\dagger + \lambda_e L e^c H_d^\dagger + \lambda_\nu L H_u \nu_R. \quad (5.5)$$

The tree-level Yukawa couplings satisfy

$$\lambda_e = \lambda_u = \sqrt{2}g_s, \quad \lambda_d = \sqrt{2}g_3, \quad \lambda_\nu = \sqrt{2}g_b \quad (5.6)$$

and we have

$$m_t = \sqrt{g_s} v \sin \beta, \quad m_b = g_3 v \cos \beta. \quad (5.7)$$

The first relation implies again a heavy top, while the bottom to tau mass ratio is now predicted, with a value $m_b/m_\tau = g_3/\sqrt{g_s} \lesssim 1$ which is apparently far from its experimental value. However, in this case, the string scale is relatively high and therefore one should take into account the renormalization group evolution above the weak scale. Solving the associated RGEs with the boundary conditions (5.7) and assuming $g_3 = \sqrt{g_s}$, we obtain acceptable m_b and m_τ masses for $M_s \sim 3 \times 10^3$ TeV and $\tan \beta \sim 80$. Note that the successful prediction of m_b and m_τ is related to the condition $m_b = m_\tau$ at the (string) unification scale, which in the case of non-supersymmetric Standard Model is obtained at relatively low energies [20]. Indeed, in Fig. 3, we plot the mass ratio m_b/m_τ as a function of the energy, within the non-supersymmetric Standard Model with two Higgs doublets. Nevertheless, the resulting value of M_s is still significantly higher than the unification

⁶ Models with similar properties have been considered in the past in the perturbative heterotic string framework.

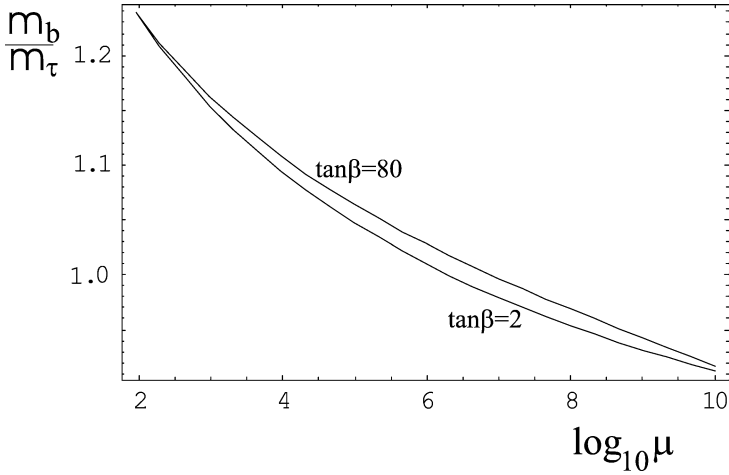


Fig. 3. Evolution of the ratio m_b/m_τ as a function of the energy μ for $\tan\beta = 2$ and $\tan\beta = 80$. We have used as low energy parameters $m_b = 4$ GeV, $m_{\text{top}} = 174$ GeV, $a_3(M_Z) = 0.12$, $\sin^2\theta_W = 0.23113$.

scale required from the analysis of gauge couplings in Section 3. Moreover, the top quark mass turns out to be rather high, $m_t \sim 220$ GeV. It is an open question whether this discrepancy can be attributed to threshold corrections that can be important in the case of two-dimensional bulk [6].

Model B'. The relevant Higgs couplings are given by

$$M_{B'} = \lambda_u Q u^c H_u + \lambda_d Q d^c H_d^\dagger + \lambda_e L e^c H_u^\dagger + \lambda_\nu L H_\nu \nu_R \quad (5.8)$$

while the tree-level Yukawa couplings by

$$\lambda_u = \sqrt{2} g_s, \quad \lambda_d = \sqrt{2} g_3, \quad \lambda_\nu = \sqrt{2} g_b \quad \text{and} \quad \lambda_e = \sqrt{2} g_2. \quad (5.9)$$

Here, as in model A, the τ and top mass are of the same order and thus in conflict with experiment. As in model A, vanishing leading order coupling could be a way out.

In the above analysis we have also assumed that only the heaviest generation acquires masses at the lowest order. The other two are considered to have vanishing trilinear Yukawa couplings. This property does not follow from the gauge symmetries we considered and should be attributed either to discrete string symmetries or to additional gauge symmetries by enlarging the model.⁶

6. Neutrino physics

One of the challenges of Standard Model extensions is the justification of the smallness of neutrino masses. The favorite scenario used to rely upon the introduction of right-handed neutrinos (SM singlets) and their mixing with some extra massive singlets. The suppression of the neutrino masses is then obtained as a result of the structure of the full mass matrix (“see-saw” mechanism). In order for this mechanism to work effectively, the extra singlet mass should be about ten orders of magnitude higher than the electroweak scale.

Among the promising features of D-brane models is a novel scenario to account for neutrino masses: right-handed neutrinos are assumed to propagate in the bulk while left-handed neutrinos, being a part of the lepton doublet, live on the brane. As a result, the Dirac neutrino mass is naturally suppressed by the bulk volume. Adjusting this volume, so that the string scale lies in the TeV range, leads to tiny neutrino masses compatible with current experimental data.

The extra-dimensional neutrino mass suppression mechanism described above can be destabilized by the presence of a large Majorana neutrino mass term. As already mentioned in Section 3, the lepton-number violating dimension five effective operator $LLHH$ leads, in the case of TeV string scale models, to a Majorana mass term of the order of a few GeV. Even if we manage to eliminate this operator in some particular model, higher order operators would also give unacceptably large contributions, as we focus on models in which the ratio between the Higgs vacuum expectation value (VEV) and the string scale is just of order $\mathcal{O}(1/10)$. The best way to protect tiny neutrino masses from such contributions is to impose lepton number conservation. As we have seen in Section 2, we can find models which successfully accommodate all SM particles and preserve lepton number as an effective global symmetry in perturbation theory. These are the models A, A' and B, B' described in detail in Section 3.

Apart from neutrino masses these theories contain also the ingredients to explain neutrino oscillations. The right-handed neutrino, being a bulk state, has a tower of Kaluza–Klein (KK) excitations. Their mixing with the ordinary (left-handed) neutrino leads to oscillation patterns that have to be compared with present solar and atmospheric neutrino data. There exist extended discussions in the literature [5] regarding the neutrino mass and oscillation problems in the context of extra-dimensional theories. Among the common results of these works is that an explanation of the solar neutrino anomaly is possible provided the small mixing angle (SMA) solution is acceptable. However, recent SNO results in conjunction with SuperKamiokande data [21–24] strongly disfavor the SMA solution and thus render this higher-dimensional oscillation mechanism problematic, at least as far as solar neutrino oscillations are concerned. A possible way out is to introduce three bulk neutrinos and explain the oscillations in the traditional way [25]. The effect of the KK mixing can be eliminated by appropriately decreasing the size of the extra dimensions and thus increasing the value of the string scale. However, all these discussions are restricted to the case of effectively one-dimensional bulk. Besides these phenomenological difficulties, there is also a serious theoretical problem, since one-dimensional propagation of massless bulk states gives rise to linearly growing fluctuations which yield in general large corrections to all couplings of the effective field theory, destabilizing the hierarchy [6].

Two-dimensional scenarios have not been considered in detail. We will see below how the above problems can be resolved and discover that a two-dimensional bulk has enough structure to describe both the solar and atmospheric neutrino oscillations by introducing a single bulk neutrino pair. On the other hand, recent experiments are also able to differentiate between the contributions of active and sterile neutrinos to the neutrino anomaly problems. From this point of view, the KK excitations do not carry any Standard Model charges and are thus considered as sterile. It is then important to examine if all these constraints are compatible with our model.

As explained in the introduction, our setup incorporates a two-dimensional bulk and we are going to assume hereby that neutrinos propagate in the full bulk volume which is a two-dimensional space. Among the common features of the models considered in Section 3, one finds tree-level neutrino couplings and mass-terms of the form:

$$\sum_{i=1}^3 \lambda_i L_i H_i \nu_R \rightarrow \sum_{i=1}^3 \lambda_i \nu_i \nu_{iL} \nu_R, \quad (6.1)$$

where i is a generation index and for each generation i , H_i is one of the available Higgs doublets H_d or H_u , providing masses to down quarks (models A, A') or to up quarks (models B, B'), respectively, with $v_i = \langle H_i \rangle$ the corresponding VEV. The above couplings provide a mass to one linear combination (ν_L) of the weak eigenstates (ν_{iL}), while the other two remain massless. Note, that it would be possible to generate masses for all left-handed neutrinos by introducing additional bulk neutrino pairs. In this case the number of free parameters is increased and predictability is lost. Thus, here, we will study the case of a single bulk neutrino pair. Defining $N_L = (\nu_L, \nu_{0L}, \nu'_{0L})$ the mass eigenstates, the weak eigenstates can be written as

$$\nu_{iL} = \sum_j U_{ij} N_{Lj}, \quad (6.2)$$

where U is a 3×3 unitary matrix with $U_{j1}^* = (U^{-1})_{1j} = \lambda_j v_j / m_D$ and $m_D^2 = \sum_{i=1}^3 \lambda_i^2 v_i^2$ is the mass-square of the massive combination (ν_L). Being of brane-bulk type, the couplings λ_i are naturally suppressed by the bulk volume v_{89} (see Section 1) and lead to a tiny Dirac neutrino mass

$$m_D = \frac{\bar{v}}{\sqrt{v_{89}}} = \frac{2\sqrt{2}}{g_3 g_2} \frac{M_s}{M_P} \bar{v}, \quad (6.3)$$

where $\bar{v} = \sqrt{\sum_{i=1}^3 h_i^2 v_i^2}$ with h_i , $i = 1, 2, 3$, the associated dimensionless Yukawa couplings and v_i the corresponding Higgs VEV ($v = \langle H_d \rangle$, $\langle H_u \rangle$) depending on the model. Using typical values for the gauge couplings (see Table 3 of Section 3), $v_i < v = 246$ GeV and $h_i / 4\pi = \mathcal{O}(1)$, we obtain $m_D < 6 \times 10^{-3}$ eV for $M_s \lesssim 10$ TeV. This provides an explanation for the smallness of neutrino masses and is actually the extra-dimensional version of the see-saw mechanism.

The above picture is simplified because we have neglected the contributions of the tower of KK neutrino states. Taking them into account, and assuming for simplicity that the two bulk radii are equal $R_8 = R_9 = R$ and form an angle $\pi/2 - \theta$, where $-\pi/2 < \theta < \pi/2$, the mass terms become

$$L_m = m_D \nu_L \sum_{\vec{k}} \delta^{-m_{\vec{k}}^2 / M^2} \nu_R^{(\vec{k})} + \sum_{\vec{k}} m_{\vec{k}} \nu_R^c(\vec{k}) \nu_R^{(\vec{k})} + \text{c.c.}, \quad (6.4)$$

where $\nu_R = \nu_R^{(0)}$ and the summation over \vec{k} extends over all KK momenta. By $m_{\vec{k}}^2$ we denote the mass-square of the KK excitation labeled by momenta $\vec{k} = (k_1, k_2)$

$$m_{\vec{k}}^2 = \frac{1}{R^2 \cos^2 \theta} (k_1^2 + k_2^2 - 2k_1 k_2 \sin \theta). \quad (6.5)$$

We also use the notation m_k^2 for the mass-square of the k th KK level. δ is a model dependent constant bigger than one, associated to the coupling of two Neumann–Dirichlet (ND) Z_2 -twisted strings to an untwisted (NN or DD) string [26]. In our models, there are four Z_2 -twisted coordinates, implying $\delta = 16$. M plays the role of an ultraviolet (UV) cutoff, which is normally the string scale M_s , but we prefer using the symbol M because in certain processes there exists an induced cutoff that can be a few orders of magnitude below M_s . For instance, this is the case of solar neutrinos, where the production energy is of order of a few MeV, and thus heavier KK modes are effectively cut off.

The mass terms (6.4) lead to a mixture of the usual left-handed neutrino with the infinite tower of its KK excitations. A detailed analysis of the eigenstate problem in our framework is presented in Appendix A where we derive the basic formulas for neutrino masses and transition probabilities. Due to its complexity, the problem can be either treated numerically in the general case or analytically using some approximation. The first approach has the disadvantage of being rather tedious as it involves summations over a very large number of KK modes, so we will adopt here an analytic perturbative approach. Concerning the interpretation of neutrino anomalies, there are also two possible treatments: the first is a direct fit of neutrino data to the transition probability formulas obtained in our framework. The second is to try to simulate the standard solutions to the solar and atmospheric neutrino anomaly problems. We will use here the second method, as it is sufficient for demonstrating the basic features of our model.

Following Appendix A, the mass spectrum of the full system, in the case of two bulk dimensions, is

$$\tilde{m}_k^2 = m_k^2 + r_k m_D^2 \delta^{-2m_k^2/M^2} (1 - \Delta_k) + \dots, \tag{6.6}$$

where r_k is the multiplicity of the k th KK level and

$$\Delta_k = \pi m_D^2 (R^2 \cos \theta) \{ \log(M^2 R^2 \cos \theta \log \delta^2) + s_k \}, \tag{6.7}$$

with s_k a volume independent constant. Our solution is based on the assumptions that $m_D R \ll 1$, as justified by (6.3) and $\Delta_n < 1$ that simplifies the formulas involved. Under these assumptions, and following the analysis in Appendix A, the survival probability for a neutrino of flavor i is given by

$$P_{\nu_i \rightarrow \nu_i} \approx 1 - 4u_i^2 (1 - u_i^2) \sin^2 \left(\frac{m_0^2 L}{4 E} \right) - 3.2u_i^2 \Delta_0 \sin^2 \left(\frac{\omega L}{R^2 4E} \right), \tag{6.8}$$

where $m_0^2 = m_D^2 (1 - \Delta_0)$ and $u_i = |U_{i1}|$ satisfying the unitarity relation $\sum_i u_i^2 = 1$; L is the distance that the neutrino travels before being detected and E is the beam energy. According to the discussion in Appendix A, the survival probability takes this form only for specific values of the angle θ :

$$\sin \theta = \frac{p}{q}, \quad p, q \in \mathbb{Z}, \quad |p| < q, \quad \omega = \frac{q(3 + (-1)^q)}{2(q^2 - p^2)}, \tag{6.9}$$

where p, q are relatively prime integers and $q = 1$ for $p = 0$. In our approximation, the survival probability (6.8) is a superposition of two modes with frequencies: $\frac{m_D^2 L}{4E}$ and $\frac{\omega L}{4R^2 E}$. These two frequencies can be considered as independent parameters, as the first

depends on the Yukawa couplings and the Higgs VEVs, while the second depends on the compactification radius or equivalently on the string scale. The existence of these two frequencies provides us with the opportunity to fit both solar and atmospheric oscillations using (6.8). Furthermore, the amplitudes of the two modes depend on u_i and Δ_0 defined in (6.7). These parameters can be used in order to fit the oscillation amplitudes.

In the standard neutrino (two flavor) scenario, one usually explains the solar neutrino anomaly by $\nu_e \rightarrow \nu_\mu$ oscillations and the atmospheric neutrino deficit by $\nu_\mu \rightarrow \nu_\tau$ oscillations. The formula for the transition probability is:

$$P_{\nu_i \rightarrow \nu_j} = \sin^2 2\theta_{ij} \sin^2 \left(\frac{\Delta m_{ij}^2 L}{4 E} \right), \quad (6.10)$$

where $\Delta m_{ij}^2 = m_i^2 - m_j^2$ is the neutrino mass difference in the case of two states mixing. Expressing L in km, E in GeV and Δm^2 in eV^2 , the frequency $\Delta m_{ij}^2 \frac{L}{4E}$ takes the form $1.27 \times \Delta m_{ij}^2 L/E$.

Recent analysis of atmospheric neutrino data [23] at 3σ c.l. gives $1 \times 10^{-3} < \Delta m_{\text{atm}}^2 < 6 \times 10^{-3} \text{ eV}^2$ and $0.7 < \sin^2 2\theta_{\text{atm}} < 1$. Regarding solar data, the situation has dramatically changed after the latest SNO results: only the LMA and LOW MSW solutions are acceptable at the 3σ c.l. with $2.3 \times 10^{-5} < \Delta m_{\text{LMA}}^2 < 3.7 \times 10^{-4} \text{ eV}^2$, $0.6 < \sin^2 2\theta_{\text{LMA}} < 1$ and $3.5 \times 10^{-8} < \Delta m_{\text{LOW}}^2 < 1.2 \times 10^{-7} \text{ eV}^2$, $0.8 < \sin^2 2\theta_{\text{LOW}} < 1$. Moreover, the LMA gives a much better fit. The region of the SMA solution (with best fit values $\Delta m_{\text{SMA}}^2 \sim 5 \times 10^{-6} \text{ eV}^2$, $\sin^2 2\theta_{\text{SMA}} \sim 2 \times 10^{-2}$) is acceptable only at the 5.5σ level and is thus practically excluded [22].

The atmospheric neutrino oscillation frequency is higher than solar solutions, $\Delta m_{\text{atm}}^2 > \Delta m_{\text{sol}}^2$, and thus we have to use the lowest frequency in (6.8) (i.e., m_0^2) to simulate solar neutrino oscillations. Formula (6.8) contains four independent parameters, namely m_D , R , M_s and u_e (assuming $u_\tau = 0$ and thus $u_e^2 + u_\mu^2 = 1$). Fitting both solar and atmospheric oscillations requires to leading order in Δ_0 :

$$\frac{\omega}{R^2} = \Delta m_{\text{atm}}^2, \quad (6.11)$$

$$m_D^2 = \Delta m_{\text{sol}}^2, \quad (6.12)$$

$$4u_e^2(1 - u_e^2) = \sin^2 2\theta_{\text{sol}}, \quad (6.13)$$

$$3.2u_\mu^2 \Delta_0 = \sin^2 2\theta_{\text{atm}}. \quad (6.14)$$

Neglecting the constant term s_0 in the expression (6.7) of Δ_0 , in the limit $MR \gg 1$, and assuming $\delta = 16$, Δ_0 can be written in terms of M_s and m_D as

$$\Delta_0 \approx \frac{1}{2\pi a^2} \frac{m_D^2 M_P^2}{M_s^4} \log \left(\frac{M_P}{\pi a M_s} \sqrt{\frac{\log \delta}{2}} \right), \quad a = \frac{2\sqrt{2}}{g_3 g_2}, \quad (6.15)$$

where we have assumed that the cutoff is equal to the string scale ($M = M_s$). This choice of the cutoff is suitable for the atmospheric neutrino data, where the oscillation amplitude is proportional to Δ_0 . In any case, the exact value of the cutoff plays a minor role in our calculation, due to the fact that it appears always logarithmically. Furthermore, the expectation value $\bar{\nu}$ is related to the rest of the parameters through Eq. (6.3), while the

angle θ enters in the Plank mass definition (1.3)

$$R^2 \cos \theta = \frac{1}{4\pi^2 a^2} \frac{M_P^2}{M_s^4}. \quad (6.16)$$

In terms of the integers p, q that have been introduced in (6.9), we can rewrite the last equation as

$$W_{p,q} \equiv \frac{3 + (-1)^q}{2\sqrt{q^2 - p^2}} = \frac{\Delta m_{\text{atm}}^2}{4\pi^2 a^2} \frac{M_P^2}{M_s^4}, \quad (6.17)$$

or equivalently

$$\cos \theta = \frac{3 + (-1)^q}{2W_{p,q}}. \quad (6.18)$$

Thus, the four conditions (6.11)–(6.14) together with (6.15) and (6.3), (6.16) fix all four parameters of the model. Therefore, fitting the atmospheric neutrino frequency (6.11), one determines the compactification radius

$$1 \times 10^{-3} < \frac{\omega}{R^2} < 6 \times 10^{-3} \text{ eV}^2, \quad (6.19)$$

or $3 < R < 6 \mu\text{m}$ for $\omega \sim 1$. Choosing for the solar neutrino deficit the preferred LMA solution, we get from the second condition (6.12) the neutrino mass range

$$4.8 \times 10^{-3} < m_D < 7.7 \times 10^{-2} \text{ eV}. \quad (6.20)$$

The third condition (6.13) fixes the mixing coefficient u_e^2 and has two possible solutions, namely, $0.18 < u_e^2 < 0.5$ or $0.5 < u_e^2 < 0.82$. Choosing $u_e^2 \simeq 0.18$ and $u_\mu^2 \simeq 0.82$ ($u_\tau = 0$), Eq. (6.14) leads to $\Delta_0 \sim 0.27$ (in the case we choose the lowest allowed value of $\sin^2 2\theta_{\text{atm}}$), which lies at the edge of the validity of our perturbative approach. Any other choice of u_i compatible with the constraints leads to bigger values for Δ_0 . This justifies also the choice $u_\tau = 0$ in order to minimize Δ_0 in (6.14).⁷ From (6.14) we get the string scale

$$8 \lesssim M_s \lesssim 13 \text{ TeV}, \quad (6.21)$$

while compatibility with (6.3) requires $\mathcal{O}(1)$ values for the Yukawa couplings. It is interesting that this range for the string scale coincides with the values we found from the analysis of gauge couplings in Section 3, for the models B and B'. Coming to the angle, we get from (6.17) $0.02 \lesssim W_{p,q} \lesssim 0.2$ for the allowed range of Δm_{atm}^2 and we can easily verify that there exist integers p, q that satisfy (6.17).

Let us now consider the LOW solution to the solar neutrino deficit. Following similar steps, the four constraints (6.11)–(6.14) in this case give

$$1.9 \times 10^{-4} < m_D < 3.5 \times 10^{-3} \text{ eV}, \quad (6.22)$$

⁷ Normally, one should repeat the eigenstate analysis of Appendix A numerically in the non-perturbative region, but from a preliminary analysis we do not expect significant change of our results.

with $u_e^2 \approx 0.28$ and thus $u_\mu^2 \approx 0.72$ and $\Delta_0 \approx 0.30$. The string scale turns out to be slightly lower in this case:

$$1.8 \lesssim M_s \lesssim 2.2 \text{ TeV}, \quad (6.23)$$

while for the angle θ we get $20 \lesssim W_{p,q} \lesssim 200$. Note that the range of string scale is now compatible with the values found from the analysis of gauge couplings in models A and A'. In this solution, the left-handed neutrino Yukawa couplings do not have to be of $\mathcal{O}(1)$.

Moreover, the practically excluded SMA solution can also be obtained in this framework. The associated parameters in this case are: $u_e^2 \sim 5 \times 10^{-3}$, $u_\mu^2 = 1 - u_e^2 \approx 1$, $\Delta_0 \sim 0.2$, $m_D \sim 2 \times 10^{-3}$ eV, $M_s \sim 6$ TeV, $0.2 \lesssim W_{p,q} \lesssim 1.2$. Note that the case $\theta = 0$ corresponds to $p = 0$, $q = 1$ and thus $W_{p,q} = 1$. As seen from our results, only the SMA solution includes this value in the allowed W -range and this is the reason why only this solution could be reproduced in the case of an orthogonal torus. The LMA and LOW solutions require a bulk forming a non-orthogonal lattice, corresponding to non-trivial values of θ . It is also worth noticing that such non-trivial values of θ induce CP violation in the neutrino sector, which is interesting to be further explored.

The mixing of the neutrino zero mode with its KK excitations can lead to a decay of the left-handed neutrino to these KK modes, considered as sterile from the SM point of view. In our framework, and to leading order in the Δ_0 expansion, the average conversion rate of a neutrino of flavor i to sterile is given by (A.19)

$$\bar{P}_{\nu_i \rightarrow s} \sim 2u_i^2 \Delta_0. \quad (6.24)$$

Constraints (6.12) and (6.14) fix both the above probabilities. Assuming the LMA solution to the solar neutrino deficit, we get

$$\bar{P}_{\nu_\mu \rightarrow s} \sim 0.44 \quad (6.25)$$

for atmospheric and

$$\bar{P}_{\nu_e \rightarrow s} \sim 0.05 \quad (6.26)$$

for solar neutrinos, where in the second case we have assumed a cutoff $M \sim 50$ MeV. For the LOW solution, the transition probabilities are similar: $\bar{P}_{\nu_\mu \rightarrow s} \sim 0.32$, $\bar{P}_{\nu_e \rightarrow s} \sim 0.08$. Note that the decay rate to sterile neutrinos is significant in the case of atmospheric neutrinos and is negligible in the case of solar neutrinos. This is related to the structure of our model for neutrino oscillations. The atmospheric neutrino deficit is simulated using the lightest KK neutrino excitation (which is interpreted from the SM point of view as a sterile neutrino), while the solar data are explained using the (active form the SM point of view) zero mode.

Constraints for the conversion of active to sterile neutrinos have been recently examined in reference [25]. Following their analysis in the case of the LMA solution, the constraint to the average decay rates for solar neutrinos is $\bar{P}_{\nu_e \rightarrow \nu_s} < 0.40$ at 90% c.l. which is obviously satisfied by our model. For atmospheric neutrinos the relative constraint takes the form

$$\Delta P = \bar{P}_{\nu_\mu \rightarrow \nu_s} - \bar{P}_{\nu_e \rightarrow \nu_s} < 0.17. \quad (6.27)$$

Evaluating this constraint in our framework, one finds $\Delta P = 0.44 - 0.10 = 0.34$ (where $\overline{P}_{\nu_e \rightarrow \nu_s} = 0.10$ in the case of atmospheric due to the higher cutoff in Δ_0 of Eq. (6.7)) which is by a factor of two higher than the experimental bound. However, one should take into consideration that our perturbative analysis, focusing on explicitly revealing oscillations, does not allow to access the region $\Delta_0 \sim 1$ where in principle the above rates could change. As mentioned earlier this region could be studied only numerically. This requires summation over a huge number of KK modes and at present it appears insoluble even numerically.

In any case the exact nature of atmospheric neutrino oscillations is expected to be further examined in the K2K [27] experiment. In case the predictive scenario of a single bulk neutrino presented here fails to satisfy the sterile production constraints, one should proceed in the introduction of additional bulk neutrinos and explain oscillations in the traditional way, that is by zero mode mass difference and not by mixing with the KKs. Their presence can still lead to sterile production which can be reduced by appropriately raising the string scale and thus decoupling the KKs [25].

7. Summary and conclusions

In conclusion, we performed a systematic study of the Standard Model embedding in type I string theory at the TeV scale. We found that the minimum configuration with interesting phenomenological features requires three sets of D-branes, so that all SM particles are obtained as open strings stretched among these brane stacks. Two of them describe respectively the strong and weak interactions, while the third one contains a single Abelian brane that extends in a two-dimensional bulk of submillimeter size.

The model predicts the correct value of the weak angle for a string scale of a few TeV. It also contains baryon and lepton number as perturbative global symmetries, ensuring proton stability and absence of large (Majorana) neutrino masses. On the other hand, it uses two Higgs doublets that can provide masses to all quarks and leptons. Concentrating on the heaviest generation, we computed all trilinear Yukawa couplings and studied the resulting mass relations. We found a naturally heavy top and the mass ratio of bottom quark to tau lepton close to its experimental value.

Finally, we have studied neutrino masses and oscillations by introducing a single right-handed neutrino state in the bulk. We found that both solar and atmospheric neutrino data can be explained if the bulk is a non-orthogonal torus forming a non-trivial angle. Solar oscillations are then explained using the zero-mode, which obtains a tiny mass from the electroweak Higgs, while atmospheric oscillations use its first KK excitation. However, in the cases of atmospheric data, it seems to be an excess in sterile production with respect to current atmospheric data analyses.

Overall, the model looks very promising and deserves further investigation. Particular directions that have not been discussed are the masses and mixing angles of the two lightest generations, possible important threshold corrections related to the two-dimensional bulk, supersymmetry breaking effects in models with brane supersymmetry breaking, as well as explicit type I string realizations.

Acknowledgements

This work was partly supported by the European Union under the RTN contracts HPRN-CT-2000-00148, HPRN-CT-2000-00122, HPRN-CT-2000-00131, HPRN-CT-2000-00152, HPMF-CT-2002-01898 and the INTAS contract No. 99 1 590. E.K., J.R. and T.N.T. would like to thank the Theory Division of CERN, J.R. the CPHT of Ecole Polytechnique and T.N.T. the L.P.T. of the Ecole Normale Supérieure for their hospitality. I.A. would like to thank Guido Altarelli for enlightening discussions.

Appendix A. Neutrino masses and oscillations

We consider the neutrino mass eigenvalue problem that arises when the usual left-handed neutrino localized on the “brane” mixes with one pair of right-handed neutrinos propagating in a two-dimensional bulk. The solution of this problem in the case of one-dimensional bulk has already been studied in the literature [5]. A new feature of the two-dimensional bulk is that the associated KK sums are divergent and a mass scale M playing the role of the UV cutoff, normally identified with M_s , appears in the mass and eigenstate expressions. Moreover, we consider neutrino oscillations and derive formulas for the transition rates of both active and sterile neutrinos.

We will assume for simplicity that the two bulk radii are equal, $R_8 = R_9 = R$, but we will allow for the possibility that the angle θ between the two compactified directions is arbitrary $-\pi/2 < \theta < \pi/2$. The masses of the KK excitations, labelled by momenta $\vec{n} = (n_1, n_2)$, are:

$$m_{\vec{n}}^2 = \frac{1}{R^2 \cos^2 \theta} (n_1^2 + n_2^2 - 2n_1 n_2 \sin \theta). \quad (\text{A.1})$$

The KK modes can be ordered according to their mass and labelled by a unique level number k . Massive levels have in general degeneracy four, apart from particular points that have higher degeneracy for special values of θ . In any case, only the direct sum of the states of each degenerate level couples to the left-handed neutrino. Hence, we can diagonalize in the degenerate subspace and choose one of the eigenstates, which corresponds to the sum of the degenerate KK modes. In this basis, the relevant neutrino mass terms take the form

$$L_m = m_{D\nu L} \sum_k \sqrt{r_k} \delta^{-\frac{m_k^2}{M^2}} \tilde{\nu}_R^{(k)} + \sum_k m_k \tilde{\nu}_R^{c(k)} \tilde{\nu}_R^{(k)} + \text{c.c.} + \text{decoupled},$$

where $\tilde{\nu}_R^{(k)} = \frac{1}{\sqrt{r_k}} \sum_{\ell} v_R^{(\ell)}$ and $\tilde{\nu}_R^{c(k)} = \frac{1}{\sqrt{r_k}} \sum_{\ell} v_R^{c(\ell)}$, $\ell = 1, \dots, r_k$, with r_k the multiplicity of the KK level with mass m_k . The mass terms can be written in matrix form ($N_L^T m N_R + \text{c.c.}$) with $N_L = (v_L, \tilde{\nu}_R^{c(1)}, \dots)$, $N_R = (\tilde{\nu}_R^{(0)}, \tilde{\nu}_R^{c(1)}, \dots)$ and m an infinite-dimensional matrix.

In order to determine the left-handed neutrino mass eigenstates, we consider

$$mm^\dagger = \begin{pmatrix} m_D^2 A & m_1 m_D \sqrt{r_1} \delta^{-\frac{m_1^2}{M^2}} & m_2 m_D \sqrt{r_2} \delta^{-\frac{m_2^2}{M^2}} & \dots & m_k m_D \sqrt{r_k} \delta^{-\frac{m_k^2}{M^2}} \\ m_1 m_D \sqrt{r_1} \delta^{-\frac{m_1^2}{M^2}} & m_1^2 & 0 & \dots & 0 \\ m_2 m_D \sqrt{r_2} \delta^{-\frac{m_2^2}{M^2}} & 0 & m_2^2 & \dots & 0 \\ \vdots & \vdots & \vdots & \vdots & \vdots \\ \sqrt{r_{k-1}} m_{k-1} m_D \delta^{-\frac{m_{k-1}^2}{M^2}} & 0 & 0 & \dots & 0 \\ \sqrt{r_k} m_k m_D \delta^{-\frac{m_k^2}{M^2}} & 0 & 0 & \dots & m_k^2 \end{pmatrix}, \tag{A.2}$$

where $A = \sum_\ell r_\ell \delta^{-2m_\ell^2/M^2}$. In the sequel we will assume that all masses are measured in string units, which we restore only at the end of our calculations.

The exact eigenvalue equation for the mass of the n th KK level \tilde{m}_n can be written in the form

$$m_D^2 \sum_\ell \frac{r_\ell \delta^{-2m_\ell^2}}{\tilde{m}_n^2 - m_\ell^2} = 1 \tag{A.3}$$

and the associated eigenstates

$$v_L^n = \frac{1}{N_n} (1, c_1^n, c_2^n, \dots) \tag{A.4}$$

with

$$c_\ell^n = \frac{m_D m_\ell}{\tilde{m}_n^2 - m_\ell^2} \delta^{-m_\ell^2} \tag{A.5}$$

and

$$N_n^2 = m_D^2 \tilde{m}_n^2 \sum_\ell \frac{r_\ell \delta^{-2m_\ell^2}}{(\tilde{m}_n^2 - m_\ell^2)^2}. \tag{A.6}$$

The above results can be used to express v_L in the basis of the mass eigenstates

$$v_L = \sum_n \frac{1}{N_n} v_L^n \tag{A.7}$$

and calculate its time evolution

$$v_L(t) = \sum_n \frac{1}{N_n} \exp\left(\frac{i\tilde{m}_n^2 L}{2E}\right) v_L^n, \tag{A.8}$$

where E is the neutrino beam energy and L is the distance from the source. Therefore, using (6.2) we can derive the time evolution of the weak eigenstates

$$v_{iL}(t) = U_{i1}v_L(t) + U_{i2}v_{0L} + U_{i3}v'_{0L}. \quad (\text{A.9})$$

The transition rate $P_{v_i \rightarrow v_j}$, that gives the probability for a neutrino of a specific flavor i produced in the source to be detected as flavor j in the detector, is

$$P_{v_i \rightarrow v_j} = |\langle v_{iL}(0) | v_{jL}(t) \rangle|^2 = \begin{cases} |1 - u_i^2 + u_i^2 T|^2, & i = j, \\ u_i^2 u_j^2 |1 - T|^2, & i \neq j, \end{cases} \quad (\text{A.10})$$

where $u_i = |U_{i1}|$ and

$$T \equiv \sum_n \frac{1}{N_n^2} \exp\left(\frac{i\tilde{m}_n^2 L}{2E}\right). \quad (\text{A.11})$$

The formulas for the transition probabilities to active neutrinos are

$$P_{v_i \rightarrow v_j} = \begin{cases} (1 - u_i^2)^2 + u_i^2(1 - u_i^2)(T + T^*) + u_i^4 |T|^2, & i = j, \\ u_i^2 u_j^2 (1 - (T + T^*) + |T|^2), & i \neq j. \end{cases} \quad (\text{A.12})$$

Therefore, the transition rate for a neutrino of flavor i to decay into a sterile neutrino is:

$$P_{v_i \rightarrow s} = 1 - \sum_{j=1}^3 P_{v_i \rightarrow v_j} = u_i^2 (1 - |T|^2). \quad (\text{A.13})$$

Using (A.11) we obtain

$$\frac{T + T^*}{2} = 1 - \frac{2}{N_0^2} \sin^2 \frac{\tilde{m}_0^2 L}{4E} - 2F_2(\tilde{m}_n^2), \quad (\text{A.14})$$

$$|T|^2 = 1 - 4F_2(\tilde{m}_n^2) + 4F_2^2(\tilde{m}_n^2 - \tilde{m}_0^2) + F_1^2(\tilde{m}_n^2), \quad (\text{A.15})$$

where

$$F_p(\tilde{m}_n^2) = \sum_{n \neq 0} \frac{1}{N_n^2} \sin^p \frac{\tilde{m}_n^2 L}{4E}. \quad (\text{A.16})$$

We can now calculate the average probabilities for a neutrino of flavor i to survive

$$\bar{P}_{v_i \rightarrow v_i} = (1 - u_i^2)^2 + u_i^2 \zeta^2, \quad (\text{A.17})$$

or to be converted to flavor j

$$\bar{P}_{v_i \rightarrow v_j} = u_i^2 u_j^2 (1 + \zeta^2), \quad i \neq j, \quad (\text{A.18})$$

or to decay into sterile

$$\bar{P}_{v_i \rightarrow s} = u_i^2 (1 - \zeta^2), \quad (\text{A.19})$$

where

$$\zeta^2 \equiv \sum_n \frac{1}{N_n^4} \tag{A.20}$$

and we have averaged over all frequency modes.

For $m_D = 0$, the eigenvalues of the matrix mm^\dagger form the usual KK tower with masses $m_{\vec{n}}$ given by Eq. (A.1). For $m_D R \ll 1$, it is natural to assume that the KK levels are slightly shifted:

$$\tilde{m}_n^2 = m_n^2 + \delta m_n^2. \tag{A.21}$$

Inserting (A.21) into (A.3) and expanding for $\delta m_n^2 \ll m_n^2 - m_{\vec{\ell}}^2, \forall n \neq \ell$, we obtain to lowest order:

$$\delta m_n^2 = \frac{r_n m_D^2 \delta^{-2m_n^2}}{1 + \Delta_n}, \tag{A.22}$$

where

$$\Delta_n = m_D^2 \sum_{\ell \neq n} \frac{r_\ell \delta^{-2m_\ell^2}}{m_\ell^2 - m_n^2} = m_D^2 \sum_{\substack{\vec{\ell} \in \mathbb{Z}^2 \\ m_{\vec{\ell}} \neq m_n}} \frac{\delta^{-2m_\ell^2}}{m_\ell^2 - m_n^2}. \tag{A.23}$$

Due to the presence of the factor $\delta^{-2m_n^2/M^2}$ (after restoring the M units), we have $\delta m_n^2 \sim 0$ for $m_n > M$, implying that KK levels above the cutoff M are not shifted. We notice also that in (A.1) we have $\frac{1}{R^2 \cos \theta} \sim \frac{M_s^4}{M_p^2} \ll M_s^2$. In this limit, we can calculate the leading terms in Δ_n :

$$\Delta_n = \pi m_D^2 (R^2 \cos \theta) \{ \log(M^2 R^2 \cos \theta \log \delta^2) + s_n \}, \tag{A.24}$$

where s_n is a constant term independent of the cutoff. Specifically, $s_0 = C$ and $s_{n \neq 0} = -\log |n_1^2 + n_2^2 - 2n_1 n_2 \sin \theta| + C$, with C a constant of order one. Similarly, for the normalization coefficients we get to the lowest order in δm_n^2

$$\frac{1}{N_0^2} = \frac{\delta m_0^2}{m_D^2} + \dots, \tag{A.25}$$

$$\frac{1}{N_n^2} = \frac{(\delta m_n^2)^2}{m_D^2 m_n^2 r_n \delta^{-2m_n^2}} + \dots. \tag{A.26}$$

The infinite KK sums F_2, F_1 in (A.14), (A.15) can in principle be calculated numerically using (A.3) and (A.6). However, this requires summation over a huge number of KK modes. A convenient approximation is to assume $\Delta_n \ll 1$ for $n > 0$. In this region

$$F_2 \sim m_D^2 \sum_{n \neq 0} \frac{r_n \delta^{-2m_n^2}}{m_n^2} \sin^2 \left(\frac{m_n^2 L}{4 E} \right) = m_D^2 \sum_{\substack{\vec{n} \in \mathbb{Z}^2 \\ \vec{n} \neq (0,0)}} \frac{\delta^{-2m_n^2}}{m_n^2} \sin^2 \left(\frac{m_n^2 L}{4 E} \right), \tag{A.27}$$

and thus, F_2 can be expressed in terms of theta-functions using the formula

$$\begin{aligned} & \sum_{\vec{n} \in \mathbb{Z}^2} \delta^{-2m_n^2} \frac{\sin^2(\beta m_n^2)}{m_n^2} \\ &= \text{Im} \int_0^\beta dx \left\{ \vartheta_3 \left(-\frac{4(x \log \delta + i)}{\pi(1 - \sin \theta)R^2} \right) \vartheta_3 \left(-\frac{4(x \log \delta + i)}{\pi(1 + \sin \theta)R^2} \right) \right. \\ & \quad \left. + \vartheta_2 \left(-\frac{4(x \log \delta + i)}{\pi(1 - \sin \theta)R^2} \right) \vartheta_2 \left(-\frac{4(x \log \delta + i)}{\pi(1 + \sin \theta)R^2} \right) \right\}, \end{aligned} \tag{A.28}$$

where $\vartheta_3(\tau) = \sum_{n \in \mathbb{Z}} e^{i\pi \tau n^2}$ and $\vartheta_2(\tau) = \sum_{n \in \mathbb{Z}} e^{i\pi \tau (n+1/2)^2}$. In the case of an orthogonal torus ($\theta = 0$), F is periodic under $\frac{L}{4E} \rightarrow \frac{L}{4E} + \pi R^2$. However, this property is lost for arbitrary values of θ . The periodicity, of the survival probability (A.10), is necessary for interpreting the neutrino anomaly through neutrino oscillations and is in general restored for rational values of the angle θ

$$\sin \theta = \frac{p}{q}, \quad |p| < q, \tag{A.29}$$

where p, q are relatively prime integers, and $q = 1$ for $p = 0$. Restricting θ to this subspace, F becomes periodic under $\frac{L}{4E} \rightarrow \frac{L}{4E} + \tau_{p,q} \pi R^2$, where

$$\tau_{p,q} = \begin{cases} \frac{q^2 - p^2}{q} & \text{for } q = \text{odd}, \\ \frac{q^2 - p^2}{2q} & \text{for } q = \text{even}. \end{cases} \tag{A.30}$$

Since F_2 is a periodic function, the next question is to compute the corresponding amplitude. To get an estimation of the amplitude we can evaluate the sum (A.27) at the half period. We get

$$F_2^{1/2} = m_D^2 \sum_{\vec{n} \in \tilde{\mathbb{Z}}^2} \frac{\delta^{-2m_n^2}}{m_n^2} = \kappa \Delta_0, \tag{A.31}$$

where $\tilde{\mathbb{Z}}^2$ is one of the sets of (even, odd) and/or (odd, odd) integers of \mathbb{Z}^2 , depending on the choice of q . More particularly, for $q = 4\ell$ with ℓ integer, $\tilde{\mathbb{Z}}^2$ is the set of (odd, odd) pairs, for $q = 2\ell + 1$, $\tilde{\mathbb{Z}}^2$ is the set of (odd, even) and (even, odd) pairs and for $q = 4\ell + 2$, $\tilde{\mathbb{Z}}^2$ is the union of the two previous sets. The constant κ takes approximately the values $\kappa \in (1/4, 1/2, 3/4)$ for each of the three cases, respectively. Moreover, an upper bound to the amplitude of F can be derived by replacing the “ \sin^2 ” terms with unity

$$F_2^{\max} = m_D^2 \sum_{\vec{n} \in \mathbb{Z}^2} \frac{\delta^{-2m_n^2}}{m_n^2} = \Delta_0. \tag{A.32}$$

Hence, the oscillation amplitude ρ lies in the range $F_2^{1/2} < \rho < F_2^{\max}$, that is $\kappa \Delta_0 < \rho < \Delta_0$ with $\kappa \in (1/4, 1/2, 3/4)$. Furthermore, we can proceed to a numerical evaluation of F for given $\sin \theta$ and MR . An explicit example is presented in Fig. 4, where we have calculated F as a function of $\frac{L}{4ER^2}$ in the case $M^2 R^2 = 10^4$, $\delta = 16$, $\sin \theta = \frac{119}{120}$. In the same figure, we have also plotted the function $\sin^2\left(\frac{240}{239} \frac{L}{4ER^2}\right)$ (gray line) with amplitude

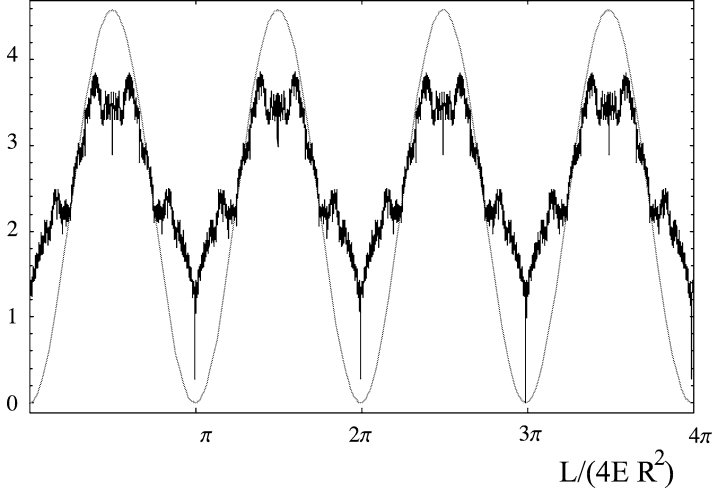


Fig. 4. Plot of the infinite two-dimensional sum $\sum_{\bar{n} \in \mathbb{Z}^2} (\delta^{-\frac{2h_{\bar{n}}}{M^2 R^2}} / h_{\bar{n}}) \sin^2(\frac{L}{4E} \frac{h_{\bar{n}}}{R^2})$ with $h_{\bar{n}} = \cos^{-2} \theta \times (n_1^2 + n_2^2 - 2n_1 n_2 \sin \theta)$ in the case $M^2 R^2 = 10^6$, $\delta = 16$ and $\sin \theta = \frac{119}{120}$. The gray line represents the dominant frequency mode $\rho \sin^2(\frac{L}{4E} \frac{240}{239R^2})$ with amplitude $\rho = 0.8 \pi \cos \theta \log(M^2 R^2 \cos \theta \log \delta^2)$.

arising from the fit to the numerical sum data. The numerical evaluation of the sum shows that the amplitude ρ can in general be approximated by $\rho \approx 0.8 \Delta_0$. Taking into account these results, we will assume in Section 6 that the KK sum F can be simulated by the dominant frequency mode

$$F_2 \approx 0.8 \Delta_0 \sin^2\left(\frac{\omega_{pq} L}{R^2 4E}\right), \quad \omega_{pq} = \frac{q(3 + (-1)^q)}{2(q^2 - p^2)}, \tag{A.33}$$

where Δ_0 is given in (A.24) and θ is given in (A.29).

Assuming $\Delta_0 \ll 1$, we can drop the terms F_2^2 and $F_1^2 < F_2^2$ in (A.15). Putting together (A.12), (A.27) and (A.33), we obtain an approximate expression for the survival probability

$$P_{\nu_i \rightarrow \nu_i} \approx 1 - 4u_i^2(1 - u_i^2)(1 - \Delta_0) \sin^2 \frac{m_0^2 L}{4E} - 3.2u_i^2 \Delta_0 \sin^2\left(\frac{\omega_{pq} L}{R^2 4E}\right), \tag{A.34}$$

where

$$m_0^2 = m_D^2(1 - \Delta_0). \tag{A.35}$$

Moreover, for the parameter ζ^2 that enters in the average transition probability formulas (A.17)–(A.19), we have

$$\zeta^2 \sim \frac{1}{N_0^4} = 1 - 2\Delta_0 + \dots \tag{A.36}$$

References

- [1] I. Antoniadis, E. Kiritsis, T.N. Tomaras, *Phys. Lett. B* 486 (2000) 186, hep-ph/0004214.
- [2] I. Antoniadis, E. Kiritsis, T.N. Tomaras, *Fortschr. Phys.* 49 (2001) 573, hep-th/0111269.
- [3] N. Arkani-Hamed, S. Dimopoulos, G. Dvali, *Phys. Lett. B* 429 (1998) 263, hep-ph/9803315;
I. Antoniadis, N. Arkani-Hamed, S. Dimopoulos, G.R. Dvali, *Phys. Lett. B* 436 (1998) 257, hep-ph/9804398.
- [4] I. Antoniadis, C. Bachas, D. Lewellen, T.N. Tomaras, *Phys. Lett. B* 207 (1988) 441;
I. Antoniadis, *Phys. Lett. B* 246 (1990) 377;
I. Antoniadis, K. Benakli, *Phys. Lett. B* 326 (1994) 69, hep-th/9310151;
J.D. Lykken, *Phys. Rev. D* 54 (1996) 3693, hep-th/9603133.
- [5] K.R. Dienes, E. Dudas, T. Gherghetta, *Nucl. Phys. B* 557 (1999) 25, hep-ph/9811428;
N. Arkani-Hamed, S. Dimopoulos, G.R. Dvali, J. March-Russell, *Phys. Rev. D* 65 (2002) 024032, hep-ph/9811448;
A.E. Faraggi, M. Pospelov, *Phys. Lett. B* 458 (1999) 237, hep-ph/9901299;
G.R. Dvali, A.Y. Smirnov, *Nucl. Phys. B* 563 (1999) 63, hep-ph/9904211;
R.N. Mohapatra, S. Nandi, A. Perez-Lorenzana, *Phys. Lett. B* 466 (1999) 115, hep-ph/9907520;
R.N. Mohapatra, A. Perez-Lorenzana, *Nucl. Phys. B* 576 (2000) 466, hep-ph/9910474;
R. Barbieri, P. Creminelli, A. Strumia, hep-ph/0002199.
- [6] I. Antoniadis, C. Bachas, *Phys. Lett. B* 450 (1999) 83, hep-th/9812093.
- [7] I. Antoniadis, E. Dudas, A. Sagnotti, *Phys. Lett. B* 464 (1999) 38, hep-th/9908023;
G. Aldazabal, A.M. Uranga, *JHEP* 9910 (1999) 024, hep-th/9908072.
- [8] D. Cremades, L.E. Ibanez, F. Marchesano, hep-th/0205074;
D. Cremades, L.E. Ibanez, F. Marchesano, *JHEP* 0207 (2002) 022, hep-th/0203160;
D. Cremades, L.E. Ibanez, F. Marchesano, *JHEP* 0207 (2002) 009, hep-th/0201205;
G. Aldazabal, S. Franco, L.E. Ibanez, R. Rabadan, A.M. Uranga, *J. Math. Phys.* 42 (2001) 3103, hep-th/0011073;
G. Aldazabal, S. Franco, L.E. Ibanez, R. Rabadan, A.M. Uranga, *JHEP* 0102 (2001) 047, hep-ph/0011132.
- [9] L.E. Ibanez, F. Marchesano, R. Rabadan, *JHEP* 0111 (2001) 002, hep-th/0105155.
- [10] R. Blumenhagen, V. Braun, B. Kors, D. Lust, *JHEP* 0207 (2002) 026, hep-th/0206038;
R. Blumenhagen, B. Kors, D. Lust, *Phys. Lett. B* 532 (2002) 141, hep-th/0202024;
R. Blumenhagen, B. Kors, D. Lust, T. Ott, *Nucl. Phys. B* 616 (2001) 3, hep-th/0107138;
M. Cvetič, P. Langacker, G. Shiu, *Nucl. Phys. B* 642 (2002) 139, hep-th/0206115;
M. Cvetič, P. Langacker, G. Shiu, *Phys. Rev. D* 66 (2002) 066004, hep-ph/0205252;
M. Cvetič, G. Shiu, A.M. Uranga, *Phys. Rev. Lett.* 87 (2001) 201801, hep-th/0107143;
D. Bailin, G.V. Kraniotis, A. Love, *Phys. Lett. B* 502 (2001) 209, hep-th/0011289;
D. Bailin, G.V. Kraniotis, A. Love, hep-th/hep-th/0210219;
C. Kokorelis, *JHEP* 0208 (2002) 018, hep-th/0203187;
C. Kokorelis, hep-th/0210200.
- [11] N. Arkani-Hamed, S. Dimopoulos, G.R. Dvali, *Phys. Rev. D* 59 (1999) 086004, hep-ph/9807344.
- [12] I. Antoniadis, M. Quiros, *Phys. Lett. B* 392 (1997) 61, hep-th/9609209.
- [13] L.E. Ibanez, F. Quevedo, *JHEP* 9910 (1999) 001, hep-ph/9908305.
- [14] I. Antoniadis, K. Benakli, M. Quiros, *Phys. Lett. B* 331 (1994) 313, hep-ph/9403290;
For a recent review see: I. Antoniadis, K. Benakli, *Int. J. Mod. Phys. A* 15 (2000) 4237, hep-ph/0007226, and references therein.
- [15] A. Sagnotti, *Phys. Lett. B* 294 (1992) 196, hep-th/9210127;
L.E. Ibanez, R. Rabadan, A.M. Uranga, *Nucl. Phys. B* 542 (1999) 112, hep-th/9808139.
- [16] E. Poppitz, *Nucl. Phys. B* 542 (1999) 31, hep-th/9810010.
- [17] I. Antoniadis, E. Kiritsis, J. Rizos, *Nucl. Phys. B* 637 (2002) 92, hep-th/0204153.
- [18] E. Kiritsis, P. Anastasopoulos, *JHEP* 0205 (2002) 054, hep-ph/0201295.
- [19] D.M. Ghilencea, L.E. Ibanez, N. Irges, F. Quevedo, *JHEP* 0208 (2002) 016, hep-ph/0205083.
- [20] H. Arason, D.J. Castano, B. Keszthelyi, S. Mikaelian, E.J. Piard, P. Ramond, B.D. Wright, *Phys. Rev. D* 46 (1992) 3945;
M.K. Parida, A. Usmani, *Phys. Rev. D* 54 (1996) 3663.
- [21] J.N. Bahcall, M.C. Gonzalez-Garcia, C. Pena-Garay, *JHEP* 0207 (2002) 054, hep-ph/0204314.

- [22] P.C. de Holanda, A.Y. Smirnov, hep-ph/0205241.
- [23] G. Altarelli, F. Feruglio, hep-ph/0206077.
- [24] A.Y. Smirnov, hep-ph/0209131.
- [25] H. Davoudiasl, P. Langacker, M. Perelstein, Phys. Rev. D 65 (2002) 105015, hep-ph/0201128.
- [26] S. Hamidi, C. Vafa, Nucl. Phys. B 279 (1987) 465;
L.J. Dixon, D. Friedan, E.J. Martinec, S.H. Shenker, Nucl. Phys. B 282 (1987) 13.
- [27] K2K Collaboration, M.H. Ahn, et al., hep-ex/0212007.